7-2014

The Delivery of Poly(lactic acid) Poly(ethylene glycol) Nanoparticles Loaded with Non-Toxic Drug to Overcome Drug Resistance for the Treatment of Neuroblastoma

Jhilmil Dhulekar
Clemson University, jdhulek@clemson.edu

THE DELIVERY OF POLY(LACTIC ACID)-POLY(ETHYLENE GLYCOL) NANOPARTICLES LOADED WITH NON-TOXIC DRUG TO OVERCOME DRUG RESISTANCE FOR THE TREATMENT OF NEUROBLASTOMA

A Thesis
Presented to
the Graduate School of
Clemson University

In Partial Fulfillment
of the Requirements for the Degree
Master of Science
Bioengineering

---

by
Jhilmil Dhulekar
July 2014

Accepted by:
Dr. Frank Alexis, Committee Chair
Dr. Daniel Whitehead
Dr. Agneta Simionescu
Dr. Jacqueline Kraveka

ABSTRACT

Neuroblastoma is a rare cancer of the sympathetic nervous system. A neuroblastoma tumor develops in the nerve tissue and is diagnosed in infants and children.[1] Approximately 10.2 per million children under the age of 15 are affected in the United States and is slightly more common in boys.[1,2] Neuroblastoma constitutes 6% of all childhood cancers and has a long-term survival rate of only 15%.[2-4] There are approximately 700 new cases of neuroblastoma each year in the United States. With such a low rate of survival, the development of more effective treatment methods is necessary.

A number of therapies are available for the treatment of these tumors; however, clinicians and their patients face the challenges of systemic side effects and drug resistance of the tumor cells. The application of nanoparticles has the potential to provide a safer and more effective method of delivery drugs to tumors.[5] The advantage of using nanoparticles for drug delivery is the ability to specifically or passively target tumors while reducing the harmful side effects of chemotherapeutics. Drug delivery via nanoparticles can also allow for lower dosage requirements with controlled release of the drugs, which can further reduce systemic toxicity.

The aim of this research was to develop a polymeric nanoparticle drug delivery system for the treatment of high-risk neuroblastoma. Nanoparticles composed of a poly(lactic acid)-poly(ethylene glycol) block copolymer were formulated to deliver a non-toxic drug in combination with Temozolomide, a commonly used chemotherapeutic drug for the treatment of neuroblastoma. The non-toxic drug acts as an inhibitor to the

DNA-repair protein present in neuroblastoma cells that is responsible for inducing drug resistance in the cells, which would potentially allow for enhanced temozolomide activity.

A variety of studies were completed to prove the nanoparticles' low toxicity, loading abilities, and uptake into cells. Additionally, studies were performed to determine the individual effect on cell toxicity of each drug and in combination. Finally, nanoparticles were loaded with the non-toxic drug and delivered with free temozolomide to determine the overall efficacy of the drugs in reducing neuroblastoma cell viability.

DEDICATION

I would like to dedicate this work to my parents, Subhash and Aparna Dhulekar, and my sister, Simrita, for their unyielding support and encouragement throughout my academic career. Without you, this achievement would not have been possible.

ACKNOWLEDGEMENTS

I would like to thank my advisor, Dr. Frank Alexis, for his guidance and support throughout my research and the completion of this thesis. I would also like to thank all the members of the Nanomedicine Lab, especially Olivia DeCroes, Stuart Grimes, Tim Olsen and Ian Hale for their help, support and friendship throughout this experience. A special thank you to Dr. Thomas Moore for his guidance and mentorship.

I am also thankful to the members of my committee, Dr. Daniel Whitehead, Dr. Agneta Simionescu and Dr. Jacqueline Kraveka.

I would also like to acknowledge the Clemson University Department of Bioengineering and our funding source INBRE.

TABLE OF CONTENTS

TABLE OF CONTENTS (CONTINUED)

Page

LIST OF FIGURES

Page

Figure

LIST OF FIGURES (CONTINUED)

Page

Figure

CHAPTER 1

GENERAL INTRODUCTION

The research presented in this thesis focuses on the treatment of Neuroblastoma, a rare cancer that affects the sympathetic nervous system. Neuroblastoma is a tumor that develops in the nerve tissue and usually occurs in infants and children.[1] It affects 10.2 per million children under the age of 15 in the United States and is slightly more common in boys.[1, 2] It is the most common type of cancer to be diagnosed within the first year of life (6% of all childhood cancers[3]) and has a long-term survival rate of only 15 percent.[2,4] There are approximately 700 new cases of neuroblastoma each year in the United States, and this number has remained roughly the same for several years.[3] The application of nanotechnology to develop safer and more effective systems for drug delivery has greatly influenced the field of oncology and is a promising approach for the treatment of cancers such as Neuroblastoma.[5] An overview is provided outlining the etiology and progression of neuroblastoma as well as the phenomenon of drug resistance is explained. Additionally, an overview of Nanomedicine, the science behind nanoparticle drug delivery and information about the specific drugs of interest is provided.

A literature review was performed to provide information on current treatment approaches for neuroblastoma and research that has been conducted on nanoparticles as drug delivery systems. The focus of this thesis remains on polymeric nanoparticles and their capacity to be effective carriers for administering chemotherapeutic drugs. The use of nanoparticles for drug delivery has the potential to significantly improve cancer therapy while reducing the harmful side effects of chemotherapeutics.

The goal of this research was to develop a novel drug delivery system for the treatment of Neuroblastomas. The aim of this project was to overcome the drug resistance of the cancer cells by encapsulating a non-toxic drug into polymeric nanoparticles that can release the drug over a prolonged period of time combined with a free toxic drug. This approach improves on the benefits of nanomedicine by passive or specific targeting of tumors, and by mitigating the effects of drug resistance. The goal was to demonstrate that co-administration of a non-toxic drug, O^6-Benzylguanine with a toxic drug, Temozolomide, lowered the drug resistance of a range of neuroblastoma cells thereby lowering the concentration of toxic drug required and enhancing the efficacy of the drug in eliminating the cancer cells. PLA-PEG- (OCH_3) nanoparticles were synthesized and drugs were encapsulated with interest for delivery to four different neuroblastoma cell lines. Free drug studies were also performed to assess the effect of the drugs individually as well as in combination to determine the optimal concentrations and time period needed for effective treatment.

This paper provides an overview of current research as well as a detailed methodology of the formulation of the polymeric nanoparticles and testing of the two drugs on a panel of neuroblastoma cells.

CHAPTER 2

NEUROBLASTOMA ETIOLOGY AND TREATMENT

2.1. Etiology

Neuroblastoma can develop in many areas of the body. It arises from the tissues that form the sympathetic nervous system, which controls body functions such as heart rate, blood pressure, digestion and certain hormone levels. This cancer starts in early nerve cells known as sympathetic neuroblasts, and can be found anywhere in this system.[3] Neuroblastomas will most commonly begin in the abdomen, in the adrenal glands, next to the spinal cord or in the chest. These neuroblastomas can spread to the bones, bone marrow, liver, lymph nodes, skin and around the eyes. In most patients, the neuroblastoma has already metastasized when it is diagnosed.[1] It is a complex and heterogeneous disease, and several factors such as age and stage of disease at diagnosis, as well as molecular, cellular and genetic characteristics of the tumor determine whether it will spontaneously regress or metastasize and become noncompliant to therapy. Sixty percent of Neuroblastomas are metastatic and are mostly diagnosed after 18 months of age.[2] Clinicians typically use a 5-year survival rate to predict treatment success. This refers to the percentage of patients who live at least five years after initial diagnosis of the cancer. The national average for the 5-year survival time is 76.4%. The five-year survival time in low-risk children is more than 90%, in children with intermediate risk is 70-90%, and only 30% in children with high-risk disease.[5] The focus of the research and experimental work presented in this thesis is on the treatment of high-risk neuroblastoma.

As mentioned earlier, most neuroblastomas are found in the abdomen and originate in the adrenal gland or sympathetic ganglia. Based on these common sites of origin and cellular features of neuroblastomas, it is generally accepted that the cells giving rise to neuroblastoma originate in the sympathoadrenal lineage of the neural crest of development. The neural crest is present during embryogenesis and gives rise to various cell types such as peripheral neurons, enteric neurons, glia, melanocytes, Schwann cells and cells of the craniofacial skeleton and adrenal medulla. The adrenal medulla is a ganglion of the sympathetic nervous system. Sixty-five percent of neuroblastomas arise in the adrenal medulla and lumbar. A small percentage of patients present a bilateral adrenal neuroblastoma suggesting that they may have a predisposing genetic lesion indicating that the bilateral tumors arise from two independent genetic lesions in the cells of the left and right sympathoadrenal lineage. It is also possible that the initiating genetic lesion occurs during early development and the tumor-initiating cells migrate bilaterally from the neural crest.[2]

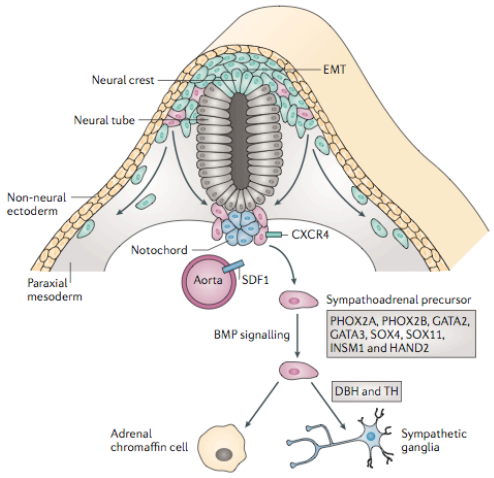

Figure 1 | Development of the sympathoadrenal lineage of the neural crest[3]

2.1.1. Familial Neuroblastoma

Children with the familial form of neuroblastoma are those with an inherited tendency to develop this cancer, and usually come from families who had one or more affected members as infants. Familial neuroblastomas are very rare, accounting for only 2% of neuroblastomas. The average age at diagnosis of familial cases is earlier than the age for sporadic (not inherited) cases. Familial neuroblastomas are likely to develop tumors in more than one organ rather than metastasizing, although metastases can occur in either familial or sporadic forms.[3] Familial neuroblastoma results from mutations in some of the signaling pathways involved in the development of the sympathoadrenal lineage. These mutations are associated with familial genetic syndromes characterized by defects in development and predisposition to neuroblastoma. The first predisposition mutation found in neuroblastoma was in paired-like homeobox 2b (PHOX2B), which codes for a homeodomain transcription factor that promotes cell cycle exit, neuronal differentiation, and has a key role in the development of neural crest-derived autonomic neurons. Another, more common lesion related to familial neuroblastoma is in the anaplastic lymphoma receptor tyrosine kinase (ALK) gene. ALK is expressed in the developing sympathoadrenal lineage of the neural crest, where it is supposed to regulate the balance between proliferation and differentiation via multiple cellular pathways, including the MAPK and RAS-related protein 1 (RAP1) signal transduction pathways. There is also evidence suggesting that PHOX2B can directly regulate ALK expression, forming a connection between these two pathways that are mutated in familial neuroblastoma. Although the ALK activating mutation F1147L contributes to

neuroblastoma tumorogenesis in mice, this specific mutation has not yet been found in familial neuroblastoma.[2]

2.1.2. Sporadic Neuroblastoma

Six to ten percent of sporadic neuroblastomas contain somatic ALK-activating mutations, and 3-4% have a high frequency of ALK gene amplification. This characteristic in both familial and sporadic neuroblastoma suggest that ALK is an oncogenic catalyst in neuroblastoma, and activation of ALK mutations or amplifications, especially in the presence of MYCN amplifications, are associated with fatal disease. The most common focal genetic lesion in sporadic neuroblastoma is the amplification of MYCN, occurring in approximately 22% of tumors. MYCN regulates proliferation, growth, differentiation and survival of cells in the developing CNS. It is expressed in the developing neural crest by several signaling pathways. Some neuroblastoma cells may contain extra copies of the MYCN oncogene, which is an indication of fast tumor progression and more difficulty in treatment.[3] Even though MYCN is a major oncogenic driver in neuroblastoma and has been studied extensively, there are no clinical trials targeting the MYCN protein directly because of the inherent difficulties in developing therapies that directly target transcription factors. Mutations in α-thalassaemia/mental retardation syndrome X-linked (ATRX) are of the most common lesions in sporadic neuroblastoma. It is suggested that ATRX functions in developmental processes, since ATRX mutations are associated with X-linked mental retardation (XLMR), but little is known about how ATRX contributes to the development or differentiation of the

sympathoadrenal lineage. Children with XLMR do not have an increased incidence of neuroblastoma, which indicates that ATRX mutations alone are not sufficient to promote tumorigenesis.[2] However, researchers have recently found that neuroblastoma cells in older children are more likely to have mutations in ATRX. Tumors with this gene tend to grow slowly, but are harder to eliminate.[3]

Cancer cells must maintain telomeres for survival, which in neuroblastoma, is typically accomplished through increased expression on telomerase. High telomerase activity is found in 30% of neuroblastomas at diagnosis and is indicative of reduced event-free survival and overall survival in multivariate analyses.[2]

2.1.3. Heterogeneity of Neuroblastoma

The heterogeneity of neuroblastoma tends to influence the individual patient response to therapy and prognosis. Heterogeneity among cancer cells in the same patient can arise in multiple ways. The most established mechanism involves the intrinsic differences among cancer cells caused by stochastic, genetic or epigenetic changes. Differences can also result from extrinsic mechanisms in which different microenvironments within a tumor present phenotypic and functional differences upon cancer cells in different locations. Further, some cancers follow a stem cell model in which tumorigenic cancer stem cells "differentiate" into non-tumorigenic cancer cells. The cancer stem cell model is not a new development, and it has been known for decades that some neuroblastomas can differentiate into a progeny that have limited proliferative potential despite retaining the oncogenic mutations of their malignant progenitors. The presence of only mature differentiated cells in residual tumor masses after chemotherapy

is a positive prognostic factor, while the presence of residual undifferentiated cells indicates disease recurrence.[8] Neuroblastomas show varying degrees of differentiation. Neuroblastomas with widespread differentiation generally have a better prognosis than those with limited differentiation. Poorly differentiated neuroblastomas are usually scattered and often fatal despite aggressive treatment. These observations have been made clinically and suggest that undifferentiated neuroblastoma cells sometimes promote disease progression.[8]

2.2. Current Research and Treatment Methods

The survival rate of all children diagnosed with high-risk neuroblastoma is less than half after 5 years of diagnosis. With such a poor success rate, the development of new agents and drug combinations is imperative to improving the prognosis for these patients.[6] By studying the tumor microenvironment, specific genes and proteins, and mechanisms of drug resistance, a lot can be understood about developing safe and effective treatment methods for neuroblastoma.

2.2.1. Current Research

Translational and clinical research for pediatric cancers is significantly different from that of adult cancers because there are comparatively few patients and drug metabolism, acute toxicities and late effects vary greatly between children and adults.[2] Recent successes in the treatment of high-risk neuroblastoma may be attributed to the use of higher doses of chemotherapy; some studies have credited the improvement to the use of myeloablative doses of cytotoxic therapy in combination with autologous bone

marrow transplantation. Relapse is common despite the achievement of remission, which further suggests that minimal residual disease is an important cause of recurrence. All-*trans*-retinoic acid (tretinoin) and 13-*cis*-retinoic acid (isotretinoin) decrease proliferation and stimulate differentiation in neuroblastoma cells, and may be effective against residual tumor cells that are resistant to cytotoxic agents.[7] Among currently marketed treatments, the delivery of anti-GD2 monoclonal antibodies has become the standard of care after two decades of research, as a result of the discovery that high-risk patients with neuroblastoma can maintain continuous remission with GD2-specific MAb therapy.[2] GD2 belongs to a unique class of T cell-independent carbohydrate antigens. However, the side effects of pain have restricted the anti-GD2 MAb dose and effectiveness has only been shown in patients with minimal residual disease and has rarely been observed in patients with bulky neuroblastoma. Early persistent minimal residual disease during immunotherapy has been highly predictive of ultimate treatment failure. Currently researched treatment strategies have been focused on immunotherapies such as vaccines to stimulate T cell-mediated immunity and adoptive T-cell therapy. Chemotherapy is common, and some children may receive neo-adjuvant chemotherapy (before surgery) or adjuvant chemotherapy (after surgery). Most chemotherapy for neuroblastoma will require a combination of drugs. The main drugs used include cyclophosphamide or ifosfamide, cisplatin or carboplatin, vincristine, doxorubicin, etoposide, topotecan, busulfan and melphalan.[3] For children in the high-risk group, larger combinations are used with higher doses, and may be followed by a stem cell transplant. The side effects of chemotherapeutic drugs can be quite destructive and debilitating, especially for a child.

For example, cyclophosphamide and ifosfamide can damage the bladder and affect fertility; doxorubicin can cause heart damage; cisplatin and carboplatin can affect the kidneys and vincristine may damage nerves.[3] For this reason, we look towards developing novel therapeutic methods such as delivering drugs via nanomaterials for direct, targeted administration in order to avoid the systemic side-effects that accompany treatment with a number of these commonly administered drugs.

2.2.2. Mechanisms of Cancer Drug Resistance

The ability of cancer cells to become resistant to a variety of drugs is known as Multiple Drug Resistance (MDR). This phenomenon is a major challenge in treating cancer because it inhibits the function of many chemotherapeutic drugs. MDR is classified as either intrinsic or extrinsic. Intrinsic MDR occurs if the tumor cell is inherently resistant to chemotherapy, and acquired MDR occurs if the tumor relapses after treatment.[9] MDR usually occurs because transporter proteins that expel drugs from cells are over-expressed on the surface of cancer cells. The expulsion of drugs lowers the therapeutic effect and cancer cells soon develop resistance to a variety of drugs.[10] MDR modulators are a group of drugs that can inhibit or reverse the processes that cause cancer cells to become resistant. A significant reason to study nanomedicine to treat cancer is because encapsulation of drugs in nanoparticles allows for co-administration of MDR modulators with chemotherapeutics. Nanoparticle-mediated delivery of these drugs lowers systemic toxicity and also evades ABC-transporter-mediated drug efflux.[9] Additionally, in order to reduce cancer drug resistance for increased therapeutic effectiveness, combination therapy has been widely adopted in clinics as a primary

cancer treatment regimen. While applying multiple drugs with different molecular targets can increase the genetic barriers that need to be overcome for cancer cell mutations, it has also been demonstrated that multiple drugs targeting the same cellular pathways could function synergistically for higher therapeutic efficacy and higher target selectivity[11]

2.2.3. Role of O^6-methylguanine DNA methyltransferase in Inducing Drug Resistance

Alkylating agents are highly reactive molecules that bind to DNA and cause cell death. The O^6 position of guanine is the most frequent site of alkylation in DNA. Alkylation at this site forms cross-links between adjacent DNA strands. The cellular DNA-repair protein O^6-methylguanine-DNA methyltransferase (MGMT) rapidly reverses alkylation at the O^6 position of guanine, thereby preventing the lethal cross-linking of the double-stranded DNA. It is through this mechanism that MGMT causes resistance to alkylating drugs.[12–14] In the absence of MGMT, O^6MeG in DNA generates point mutations and DNA double-strand breaks via cellular replication and DNA mismatch repair (MMR) that trigger cell death by apoptosis.[37] It is known that MGMT is widely expressed in all types of neuroblastoma and plays a key role in causing drug resistance in the cancer. MGMT expression is primarily dependent on the methylation status of the gene, that is, the presence of 5-methylcytosine in specific CpG islands of the *mgmt* promotor. Regulation of MGMT expression is directed mainly via promotor methylation. 97 CpG islands have been identified in the *mgmt* promotor.[37]

Because of the significant impact MGMT has on cancer formation and therapy effectiveness, it is well suited to be used as a biomarker. Therefore, there are specific

methods for determining the MGMT levels of normal and cancerous tissues. These methods include assays for MGMT activity, MGMT promoter methylation and MGMT protein by immunohistochemistry (IHC). MGMT activity assays calculate the number of active molecules per unit protein or DNA. This can be measured in homogenates from fresh or frozen tumor tissue. This is expressed in fmol per mg protein, per μg DNA or per cell number. MGMT activity corresponds with the MGMT protein and RNA level. Another method is promoter methylation specific PCR (MSP), which is used to detect promoter methylation. DNA methylation is a crucial mechanism for epigenetic gene regulation and plays a significant role in carcinogenesis. Methylation of the CpG islands of the *mgmt* promoter correlates with the loss of MGMT protein expression in tumor tissue. Next, IHC allows determination of MGMT protein levels on sections from frozen or paraffin embedded tumor tissue. Using specific antibodies and colorimetric/fluorescent dyes to detect MGMT allows for semi-quantitative protein assessment. Histological analysis can identify heterogeneous areas within a tumor and distinguish tumor cells from non-neoplastic tissue. In a study conducted on methylation mechanisms in primary colorectal cancers, it was shown that tumors containing a methylated promoter show lower MGMT protein expression and activity than the non-methylated tumors.[37,38] MGMT status, as defined by activity, promoter methylation and protein level, is currently regarded as a reasonable biomarker for predicting normal cell response to alkylating carcinogens and the tumor's response to O^6-tumor-therapeutic drugs.[37]

There is high variability of MGMT activity between different tissues. Also, not only does MGMT activity differ between different tissues, it also differs between individuals and between different stages of development. In general, brain cancer has low MGMT expression, which explains the relative sensitivity of nervous system cancers to methylating anti-cancer drugs like TMZ.[37] The comparison of MGMT activity in normal and neoplastic human brain samples has been reported in various studies. In general, the values for normal brain and primary brain tumors are similar and vary up to 40-fold in normal tissue and 100-fold for tumors. Due to the high levels of variation of MGMT levels, it is possible that large changes in MGMT are associated with tumorigenesis and that these changes affect response to treatment with alkylating agents. For example, decrease in MGMT activity increases sensitivity to alkylating agents while elevation of MGMT results in resistance to these agents. Silber et. al assayed MGMT activity in 60 human brain tumors overlying 25 of these tumors with histologically normal brain samples to determine whether MGMT content varied with diagnosis and patient characteristics. Their results revealed large variation in MGMT content in individual samples as well as in mean MGMT levels between specific tumor types. Mean tumor and normal brain MGMT levels did not vary between males and females, however MGMT levels in both neoplastic and normal tissue decreased with age. In Silber's experiment, the 60 tumor specimens were found to be highly heterogeneous in MGMT content, with a range from <0.5-104.1 fmol/10^6 cells. Tumor MGMT was higher in patients under 20 years of age than in those older than 20 years.[33] In another study with pediatric brain tumors, MGMT activity was found to be 5-fold higher in children between

3 and 12 years than in infants and adolescents.[37,39] Furthermore, a second study found 9-fold higher MGMT activity in tumors versus normal brain.[37] No strong correlation was found between the fraction of cells in S phase and MGMT activity, suggesting that the proliferative state of human brain tumors is not predictive of MGMT levels. Studies with cultured cells have shown that proliferating cells have enhanced levels of DNA repair activities. This, along with the finding that there is no correlation between the fraction of tumor cells in S phase and MGMT activity, demonstrates that the inter-individual variation of tumor MGMT activity is not due to differences in the fraction of proliferating cells. Furthermore, it indicates that elevated MGMT levels accompanying tumorigenesis is not a result of tumors containing greater numbers of proliferating cells than normal brain.[33]

Repair mediated by MGMT is unique compared with other DNA repair pathways. This is because MGMT repair (1) acts alone without relying on any other proteins or cofactors; (2) transfers the alkyl group to an internal cysteine residue in the protein, acting both as a transferase and an acceptor of the alkyl-group; (3) it inactivates itself after receiving the alkyl-group from guanine, and is therefore a suicidal protein; (4) it repairs in a stoichiometric fashion.[34] The level of MGMT varies greatly according to the type of tumor and also varies among same type of tumors. The MGMT gene is not usually mutated or deleted, therefore a lack of MGMT may be caused by changes that do not alter the genetic information of the cell. DNA methylation is the main type of epigenetic modifications in humans, and plays an important role in tumorigenesis.[12]

MGMT is a relatively stable protein, with a half-life greater than 24 hours. There is evidence that phosphorylation of MGMT affects its activity.[15,16]

Repair by MGMT does not involve excision of the alkylated base from DNA; it is a one-step reaction in which the methyl or chloroethyl group at the O^6 position of guanine is transferred to the cysteine residue in the active center of the MGMT molecule.[16–18] This results in restoration of guanine in the DNA and irreversible inactivation of MGMT; therefore, MGMT is often referred to as a "suicide enzyme."[16]

Repair capacity is initially determined by the number of active MGMT molecules in a cell and, if damage levels exceed the levels of pre-existing molecules, the rate of de novo synthesis following inactivation. Protection against cell death is a linear function of MGMT activity up to MGMT levels of approximately 200,000 molecules per cell, above which the toxicity of other lesions becomes dominant. Some evidence suggests that after alkyl group transfer, MGMT undergoes ubiquitination and proteosome-mediated degradation.[16]

No other functions of MGMT have been described. In adherent cells, no effect on cell growth is observed whether they express low or high levels of MGMT. This indicates that MGMT is not linked to regulation of proliferation. Additionally, although MGMT is often up-regulated in cells of more aggressive tumors, there is no evidence that MGMT has a direct stimulator or inhibitory effect on tumor growth.[16] Interestingly enough, however, a compilation of data exhibits that the normal brain tissue of brain tumor patients shows lower MGMT activity than that of non-tumor patients. This finding

suggests that individuals with low MGMT activity in the brain are more prone to brain tumor formation.[37, 39]

Only limited data is available comparing MGMT expression, activity and clinical outcome. In one study with newly diagnosed or recurrent glioma, 24% of tumors lacked detectable MGMT activity. In another study comparing the clinical outcome of combined radiotherapy/TMZ therapy in glioblastoma patients expressing low and high MGMT activities, there was a better therapeutic response when the pretreatment tumor expressed below 30 fmol/mg protein activity compared to patients expressing MGMT above this point.[37]

2.2.4. Application of O^6-Benzylguanine for Inhibition of MGMT

Recent research indicates that it may be possible to increase the sensitivity of resistant tumors with the use of agents that inhibit MGMT. One such inhibitor is O^6-benzylguanine (O^6-BG); it is a substrate for MGMT that inactivates the enzyme. O^6-BG has been shown to enhance the response to alkyl nitrosoureas in vitro and in vivo.[12] O6-BG reacts with MGMT by covalently transferring the benzyl group to the active site, cysteine, and causes an irreversible inactivation of the enzyme. Alone, O6-BG is not toxic, but it induces tumor cells to be 2- to 14-fold more sensitive to alkylating agents in the *in vitro* and *in vivo* settings. This establishes the potential of O6-BG as a therapeutic enhancer of these drugs.[34] Complete inactivation of MGMT activity was observed as early as 15 minutes after addition of O^6-BG to culture medium.[16,19] O^6-BG has remained the most extensively used agent for experimental purposes and in pre-clinical and clinical trials due to its promising properties. In initial pre-clinical experiments, pre-treatment

with O^6-BG increased carmustine sensitivity in athymic mice bearing either human medulloblastoma or human glioblastoma xenografts, showing regression of 18/20 xenografts. In recent phase I clinical trials, it was determined that in adult patients, O^6-BG doses of 100 mg/m^2 to 120 mg/m^2 are necessary for complete inactivation of MGMT.[16,20,21] Furthermore, the maximal dose of TMZ was found to be 470 mg/m^2, given with this dose of O^6-BG.[34] In phase I trials with O^6-BG in children suffering from CNS tumors, the maximal tolerated dose of TMZ given 30 minutes after infusion of 120 mg/m^2/day O^6-BG for 5 consecutive days was 100 mg/m^2/day.[16,22] Antitumor activity was observed at 120 mg/m^2/day O^6-BG combined with TMZ doses greater than 55 mg/m^2/day.[17] These results are promising indicators for the CNS tumor models tested, which suggest that the combination treatment of Temozolomide and O^6-Benzylaguanine on neuroblastoma tumor models should show similar results.

2.2.5. Treatment of Neuroblastoma with Temozolomide and O^6-Benzylguanine

Temozolomide (TMZ) is a new generation drug, commercially known as Temodal, or Temodar®.[17] It is DNA methylating imidazole tetrazinone that inhibits cell growth in neuroblastoma.[23] This drug does not need metabolic activation and decomposes spontaneously into its active form, methyltriazenoimidazole carboxamide (MITC), which releases carbonium ions that alkylate DNA. It has recently been shown that apoptosis occurs in the 2nd, 3rd and 4th cell cycle following treatment with TMZ.[17] Phase I studies in adults and children determined the maximum tolerated dose as 200 mg/m^2/d for five days. Myelosuppression is the dose-limiting toxicity of TMZ and other O^6-alkylating drugs. For TMZ, myelosuppression occurred at a total dose of 1.25 g/m^2 and was

reversible and noncumulative. According to recent studies, continuous TMZ administration allows dose escalation from 1,000 to 2,100 mg/m^2 over 28 days and causes prolonged MGMT depletion, but such clinical studies have not been conducted yet on children.[24] It was shown that 7% of patients had grade 3 or 4 hematological toxic effects following concomitant radiotherapy and TMZ, and 14% following adjuvant TMZ.[17] The cytotoxic activity of TMZ is mediated through reactive O^6-methylguanine in DNA, therefore, inhibition of MGMT may increase the cytotoxicity of TMZ against neuroblastomas.[25]

The high level of MGMT expression is one recognized mechanism of TMZ resistance. This DNA repair protein removes methyl adducts placed on DNA by TMZ, thereby reversing the cytotoxic effects of the drug.[6] The mechanism of the toxic effect of O^6-alkylating agent, in the majority of situations, suggests that repair by MGMT almost completely inhibits cell death, particularly in the lower dose range of the agents.[17] Sensitivity to TMZ appears to be inversely related to levels of MGMT expression, which can be quantified directly at the protein level by immunohistochemistry analysis of tumor tissue, or indirectly by assessing methylation of the promoter that regulates MGMT expression because hypermethylation silences the expression of this gene. It has been shown that patients whose tumors express high levels of MGMT would fail TMZ therapy.[6] In glioma cells in vitro, MGMT is recovered within 1-2 cell cycles following a single TMZ treatment, but this effect will be dose and cell line dependent.[17]

Another known mechanism of resistance to TMZ is decreased or nonexistent expression of the mismatch repair proteins MSH-2 and MLH-1. In the presence of

methylating agents such as TMZ, it is theorized that these repair enzymes engage in recurring attempts to repair DNA lesions, generating a chronic strand break condition that induces apoptosis. Therefore, the presence of an intact mismatch repair system seems to be necessary for TMZ cytotoxicity. However, reports indicate that this mechanism of resistance is uncommon in neuroblastoma.[7]

Given the availability of the MGMT-inactivating agent, O^6-Benzylguanine (O6-BG), MGMT could be a relevant therapeutic target due to its wide expression in neuroblastoma. O^6-BG has been shown in single-agent clinical studies to effectively inactivate MGMT activity in tumor tissue. Further, in pre-clinical experiments, pre-treatment with O^6-BG significantly improved the activity of TMZ against various tumors with a range of MGMT activity as a result of depleting MGMT protein.[7] Pre-treatment with O^6-BG (35 mg/kg) completely eliminated MGMT activity in mice bearing human melanoma xenografts, and the combination of TMZ (40 mg/kg) administered together with O^6-BG on five consecutive days produced a significant tumor growth delay in comparison to TMZ alone.[16] Phase II trials are currently in progress in adults and children with brain tumors to evaluate the clinical activity of O6-BG combined with TMZ.[7] In the case of metastatic neuroblastoma xenografts, combined TMZ/Irinotecan (IRN) therapy with O^6-BG enhanced the survival of mice by from 10% to 56%.[7,17] This drug has been clinically shown to effectively inactivate MGMT activity in tumor tissue. Friedman et al. observed the drug combination of O^6-BG-TMZ-IRN in a murine model of malignant glioma expressing MGMT. They found that the three-drug combination delayed tumor growth by a median of >150 days compared to <37 days for each drug

alone. Based on this data, tumors with higher sensitivity to TMZ would express little MGMT but retain MLH-1 and MSH-2. In tumors with high MGMT expression coupled with a mismatch repair system, pre-treatment with O^6-BG should increase sensitization to TMZ.[7]

In an *in vitro* study conducted by Wagner et. al, MGMT expression was detected in 88% of neuroblastoma tumor samples by immunohistochemistry. There was variation of >40% in only 6 (8%) of the tumors, which is likely related to the heterogeneous expression of MGMT within a single tumor. There was no correlation between disease stage and level of MGMT expression. It was concluded that the majority of primary neuroblastoma cell lines express MLH-1, MSH-2 and MGMT. These results indicated that expression of MGMT might be the more common mechanism of resistance to TMZ in neuroblastoma cells.[7]

In an assessment of the effect of O6-BG on the sensitivity of neuroblastoma cell lines to TMZ, 25 μmol/L of O6-BG, which has previously been shown to inactivate MGMT, was added to the cell cultures 24 hours prior to addition of varying concentrations of TMZ. The data showed that O6-BG sensitized the cells to TMZ by 11- to 12-fold. It was also demonstrated that O6-BG reduced the IC_{50} of TMZ by approximately 10-fold.[7]

CHAPTER 3

POLYMERIC NANOPARTICLES AND APPLICATION TO CANCER TREATMENT

3.1 Nanotechnology and Nanomedicine

Nanotechnology is defined as the understanding and control of matter in the 1-100 nm dimension range. Nanomedicine is the application of nanotechnology to medicine, and involves the use of engineered materials at this scale to develop novel therapeutic and diagnostic modalities. The use of nanomaterials provides the ability to modify properties such as solubility, diffusivity, blood circulation half-life, drug release characteristics, and immunogenicity. The last two decades have seen a rapid growth in the development of nanoparticle-based therapeutic and diagnostic agents for the treatment of cancer, diabetes, pain, asthma, allergy, infections, etc. These nanomaterials may provide more effective and convenient routes of administration, lower therapeutic toxicity and eventually reduce health-care costs. Nanoparticles allow targeted delivery and controlled release as therapeutic delivery systems.[26] Commonly recognized nanoparticle vectors include: liposomes, micelles, dendrimers, solid lipid nanoparticles, metallic nanoparticles, semiconductor nanoparticles, and polymeric nanoparticles.[9] There are many advantages of nanoparticle-based drug delivery systems; these include: (1) the ability to improve the solubility of poorly water-soluble drugs, (2) prolonged half-life of drug systemic circulation by reducing immunogenicity, (3) sustained release of drugs thereby lowering frequency of administration, (4) delivery of drugs in a target manner to minimize systemic side effects, (5) delivery of two or more drugs simultaneously for combination therapy for increased efficacy, and (6) delivery of drugs across a range of biological

barriers including epithelial and endothelial. Additional advantages of nanoparticles include specific binding of drugs to targets in cancer cells, visualization of tumors using various imaging modalities, and optimized dose scheduling for improved patient compliance.[27] More than 20 nanoparticle therapeutics have been approved by the FDA for clinical use and numerous nanoparticle products are currently under clinical testing for various applications.[26-28]

3.2 Nanoparticles for Cancer Treatment

The search for a successful cancer treatment depends on the discovery of the ultimate therapeutic and delivery method. Traditional treatment options such as chemotherapy and radiation have made significant advances over the past decades, however, cancer therapy is still not completely optimized. The effectiveness of cancer therapy depends on a fine line between the ability of the therapeutic to eliminate the tumor while minimizing the negative affect on healthy cells. Systemic administration of bolus doses of powerful chemotherapeutics often results in severe side effects due to the action of the drugs on sites other than the intended target. With this nonspecific drug action, the concentration of the drug that can be available at the tumor site itself may be below the minimal effective concentration, resulting in a difficult dilemma between choosing a near-toxic effective dose and a comfortable ineffective dose. Further, intravenous injection of toxic agents introduces a serious threat to healthy tissues and leads to dose-limiting side effects.[11] As a result, decades of research have focused on developing cancer-specific drugs and delivery systems that can preferentially localize therapeutic agents to the tumor site.[9]

Nanoparticles are effective tumor-targeting vehicles because of the unique innate property of solid tumors. Solid tumors undergo rapid growth and as a result typically have fenestrated vasculature and poor lymphatic drainage, causing an enhanced permeability and retention (EPR) effect.[27] Rapid and defective angiogenesis causes increased permeability of the blood vessels in tumors.[10] This property allows nanoparticles to accumulate specifically at the tumor site. Blood vessels in tumors are irregular in their structure compared to those in normal tissues. Tumor vessels are heterogeneous in their distribution, dilated and tortuous, and leave avascular spaces of varying sizes. The tumor vessel-wall structure is characterized by wide inter-endothelial junctions, an abnormally thick or thin basement membrane, leakiness and hyper-permeability in some areas and maximum pore diameters of several hundred nanometers.[27]

The elevated viscous and geometrical resistance of the vasculature can compromise tumor blood flow. As a result, the average velocity of red blood cells (RBCs) in tumor vessels can be significantly lower than in normal vessels and the overall perfusion rates in tumors are also lower compared with normal tissues. Blood velocity in tumors is independent of vessel diameter and unevenly distributed, creating poorly perfused or un-perfused regions. The presence of these un-perfused regions results in a hostile tumor microenvironment, which is characterized by low partial oxygen pressure, low pH and necrotic tissue, which contributes to drug resistance and tumor progression. Furthermore, functional lymphatic vessels only exist in the tumor periphery. These peritumor lymphatics transport fluid, growth factors, cancer cells, and mediate tumor

metastases via the lymphatic network. The inefficiency of fluid drainage from the tumor center along with fluid leakage from tumor vessels contributes to interstitial hypertension.[27] Consequently, the dysfunctional lymphatic drainage in tumors retains the accumulated nanoparticles and allows them to release drugs in the vicinity of the tumor cells.[11] Nanoparticles protect the drug from rapid metabolism and clearance, as well as preventing uptake by the reticuloendothelial system and mononuclear macrophages. Nanoparticles thus have the ability to circulate for prolonged periods of time, allowing them to eventually reach the tumor vasculature where, with the aid of the EPR effect, they specifically extravasate through the fenestrated capillaries to accumulate drugs at the tumor mass. Further, at the tumor site, nanoparticles can be endocytosed/phagocytosed therefore enhancing cell internalization of the drug and leading to delivery of the drug closer to the intracellular site of action.[9] Transport of a therapeutic agent from the systemic circulation to cancer cells is a three-step process: First, nanoparticles flow to different regions of tumors via blood vessels. Then, they must cross the vessel wall, and finally, penetrate through the interstitial space to reach the target cells. The elevated interstitial fluid pressure (IFP) resulting from the interstitial hypertension reduces convective transport, while the dense extracellular matrix hinders diffusion. This brings a challenge to delivering drug-loaded nanoparticles because this interstitial hypertension and defective blood supply reduces the efficacy and delivery of the therapeutic agents to solid tumors. Subsequently, hypoxia in tumor cells induces resistance to chemotherapy as well as resistance to several cytotoxic drugs. As a result, strategies to enhance drug delivery have focused on normalizing the tumor vasculature to increase the efficiency of

the vascular network, and normalizing the tumor interstitial matrix, so that nanoparticles penetrate faster and deeper inside the tumor. For optimal efficiency, the therapeutic agent must reach tumors in sufficient amounts to kill cancer cells but at the same time not adversely affect normal tissues. In this case, the smaller the particles the better the transport, however, small molecules such as chemotherapeutics generally extravasate in normal tissues, which may cause adverse effects. The size of the particles also affects their circulation time in the blood stream; as long as the therapeutic agent is not toxic to normal tissues, it makes sense to prolong its half-life in the blood. Therefore, the size of the particle must be optimized for each tumor and its metastases.[27] In addition to size, the surface charge of the nanoparticle also plays a crucial role in extravasation and interstitial transport. Cationic nanoparticles have been shown to preferentially target tumor endothelial cells and exhibit higher vascular permeability than their neutral or anionic counterparts. Neutral nanoparticles diffuse faster and distribute more homogeneously inside the tumor interstitial space than cationic and anionic particles, because the latter form aggregates with negatively or positively charged molecules. Transport of nanoparticles through the interstitial matrix is governed by diffusion and convection, as shown in the equation below:

$$(\partial C_i/\partial t)+v\nabla C=D\nabla^2 C_i+R$$

Figure 2 | Mathematical model describing transport of nanoparticles through the interstitial matrix.[27]

Where C_i is the nanoparticle concentration, v the interstitial fluid velocity, D the diffusion coefficient of the nanoparticles and R that accounts for binding or degradation of the

nanoparticles. The fluid velocity depends on changes in the interstitial fluid pressure and the diffusion coefficient depends on the nanoparticle properties (size, charge, configuration) and the structure of the interstitial matrix.[27]

3.3 Polymeric Nanoparticles

It has been shown that nanoparticle and polymer conjugate delivery can allow concentrations of the drug near the tumor site to reach 10- to 100-fold higher than when administering free drug.[9] As a result, many of the nanoparticle therapeutics currently in clinical and preclinical investigations are polymeric nanoparticles. Polymeric nanoparticles are engineered from biocompatible and biodegradable polymers. Most of these nanoparticles are formulated using block-copolymers consisting of two or more polymer chains with different hydrophilicity. These copolymers spontaneously assemble into a core-shell structure in an aqueous environment. The hydrophobic blocks form the core to minimize the exposure to aqueous surroundings while the hydrophilic blocks form the shell to stabilize the core. This creates a structure that is well suited for drug delivery. The hydrophobic core can carry therapeutics with high loading capacity while the hydrophilic shell provides steric protection for the nanoparticle.[28] Polymeric nanoparticles are identified by their morphology and polymer composition in the core and corona.[36]

The therapeutic load can be conjugated to the surface or encapsulated inside the core.[36] Polymeric nanoparticles can be formulated to encapsulate either hydrophilic or hydrophobic small drug molecules. These structures have a diameter typically ranging from 10 to 100 nm.[29] The drug delivery systems can be designed to deliver controlled

release or a triggered release of the therapeutic. The most important characteristics of nanoparticles are their size, encapsulation efficiency, zeta potential, and release characteristics. Nanoparticles have an advantage over larger microparticles because they are better suited for intravenous delivery. The smallest capillaries in the body are 5-6 μm in diameter; consequently, the size of particles being circulated in the bloodstream must be significantly smaller than 5 μm, without forming aggregates to ensure that the particles do not form an embolism.[7]

The most commonly used polymers for nanoparticles are poly(lactic acid) (PLA), poly(glycolic acid) (PGA), and poly(lactide-co-glycolide) (PLGA). These polymers are known for their biocompatibility and resorbability through natural mechanisms[8]. Polyethylene glycol (PEG) has also been widely used to enhance the pharmacokinetics of nanoparticle formulations. PEG is a highly hydrated flexible polymer chain that limits plasma protein adsorption and biofueling of nanoparticles while reducing renal clearance of relatively smaller drug molecules, thereby prolonging drug circulation half-life. PEG is also non-toxic and non-immunogenic, which makes it appropriate for clinical applications.[7] In fact, PLA-PEG and PLGA-PEG nanoparticles for delivery of anticancer drugs have been approved outside the United States and are in late-phase clinical trials within the United States.[30] Natural polymers such as proteins or polysaccharides have not been widely used for the purpose of nanoparticle drug delivery since they vary in purity and often require cross-linking which could denature the embedded drug. Many protocols exist for synthesizing nanoparticles based on the type of drug used and the desired delivery route. Once a protocol is chosen, the parameters must be adjusted to create the

best characteristics for the nanoparticles.[7] The most common method for preparation of solid, polymeric nanoparticles is the emulsification-solvent evaporation technique, a method that is effective for encapsulating hydrophobic drugs.[8] PLA-PEG is an amphiphilic polymer that s flexible in solution and it contains free amino and carboxyl groups that ionize and interact in water. These characteristics allow it to self-assemble and encapsulate chemicals via hydrophobic/hydrophilic and electrostatic interactions.[31] The chain length, shape and density of PEG on the particle surface have been considered to be the main parameters affecting nanoparticle surface hydrophilicity and phagocytosis.[36] The primary reason for preparing PEG functionalized particles is to improve the long-term systemic circulation of the nanoparticles. PEG functionalized particles are not recognized as foreign bodies and are not taken up by the body, allowing them to circulate longer providing for a sustained systemic drug release. Due to this behavior, and their ability to prevent protein absorption, PEG functionalized nanoparticles are often called "stealth nanoparticles."[36,7]

There are numerous known barriers that exist in the human body to protect it from foreign particles. These barriers include cellular and humoral branches of the immune system as well as mucosal barriers. Nanoparticles are well suited to overcome these barriers to reach their target due to their unique size, and ability to accept surface functionalization to incorporate desired characteristics.[36] The next phase of research in nanoparticle systems involves the addition of targeting ligands such as antibodies, peptides, and aptamers, which may further improve efficiency and reduce toxicity.[26]

3.4 Drug Encapsulation & Release Characteristics

Drug loading into polymeric nanoparticles can be achieved by three techniques: (1) the drug is covalently attached to the polymer backbone, (2) the drug is adsorbed to the polymer surface, or, (3) the drug is entrapped in the polymer matrix during preparation of the nanopartices.[32] In the latter method, drug encapsulation is achieved by mixing the drug with the polymer solutions during a solvent displacement technique. A water-miscible solvent such as acetonitrile is used to dissolve the hydrophobic drugs together with the di-block copolymers. The solution is mixed with water. The organic solvent diffuses into the aqueous phases and evaporates, and the hydrophobic polymers self assemble to form nanoparticles with drugs encapsulated inside.[11] The molecular weight and concentration of the polymer used affects the nanoparticles. The molecular weight of the polymer has opposite effects on nanoparticle size and encapsulation efficiency. Smaller nanoparticles can be prepared with lower molecular weight polymer, however, resulting in reduced drug encapsulation efficiency. Conversely, a higher polymer concentration increases encapsulation efficiency and size of nanoparticles.[8] As emphasized earlier, particle size and encapsulation efficiency are two of the most important characteristics of nanoparticles for drug delivery applications. It is necessary to determine what the goal of the nanoparticle delivery system is before deciding on the desired size. For example, if the goal is rapid dissolution in the body then the particle size should be approximately 100 nm or less. If prolonged dissolution is desired, larger particles around 800 nm are preferred. That said, encapsulation efficiency increases with the diameter of the nanoparticles.[7]

Several factors affect the release rate of the entrapped drug. Larger particles have a smaller initial burst release and longer sustained release than smaller particles. Additionally, greater drug loading leads to greater burst and faster release rate.[11] For example, in a study conducted by Leroux et. al, PLA nanoparticles containing 16.7% savoxepine released 90% of their drug load, while particles containing 7.1% savoxepine released their content over 3 weeks. The initial burst release is believed to be caused by poorly entrapped drug, or drug adsorbed onto the outside of the particles.[7] Polymeric nanoparticle drug delivery systems are relatively stable *in vivo*, and can employ both controlled or triggered release of drugs.[11]

Compared to other nanomaterials, polymeric nanoparticles have higher stability, sharper size distribution, more tunable physicochemical properties, sustained and more controllable drug-release profiles, and higher loading capacity for poorly water-soluble drugs.[11] As a result of these properties, PEG-PLA nanoparticles are suitable carriers for therapeutics to (1) minimize the drug resistance of the cancer cells and (2) allow for effective treatment of the cancer by the specific drug of interest. This forms the basis of the experimental work presented in this thesis.

CHAPTER 4

FORMULATION AND DELIVERY OF O^6-BENZYLGUANINE LOADED PLA-PEG-(OCH_3) NANOPARTICLES I2N COMBINATION WITH TEMOZOLOMIDE

4.1 Introduction

The goal of this research was to develop a polymeric nanoparticle drug delivery system for the treatment of high-risk neuroblastoma. In order to enhance the efficacy of

the therapeutic drug Temozolomide, it was necessary to overcome the drug resistance of the neuroblastoma cells by inhibition of MGMT. To develop this drug delivery system, PLA-PEG-(OCH_3) nanoparticles were synthesized and encapsulated with the non-toxic MGMT inhibiting agent, O^6-Benzylguanine. These drug-loaded nanoparticles were co-administered with the toxic therapeutic Temozolomide (TMZ). Concentrations of TMZ were varied while keeping nanoparticle and O6-BG concentrations constant and incubation periods of 24, 48 and 72-hours were tested.

To prove that the O6-BG loaded nanoparticles and the nanoparticles themselves were non-toxic, the cells were also treated with drug-loaded and unloaded nanoparticles. PLA-PEG-(OCH_3) nanoparticles were synthesized and delivered to cells at varying concentrations and incubation periods of 24, 48 and 72-hours. O6-BG was loaded into the nanoparticles at 2 mg/mL. Nanoparticle concentration was varied to determine the optimal concentration that can be administered without causing toxicity.

It was also necessary to test the effect of the individual drugs on cell viability. Free O^6-BG, free TMZ and combination free O^6-BG + TMZ toxicity studies were conducted. 3 types of free drug combination studies were conducted to vary the concentrations of both drugs, either holding TMZ constant and varying O^6-BG or holding O^6-BG constant and varying TMZ. The results of these studies were used to determine the optimal concentration of each drug that did not exceed desired toxicity levels. These optimal concentrations were later used to determine the drug concentrations needed for drug-nanoparticle combination studies.

Lastly, to confirm that the nanoparticles were indeed uptaken by the cells, a fluorescent NP uptake study was performed. Alexa Fluor 647 cadaverine was conjugated with PLA to formulate a fluorescent polymer. This polymer was then conjugated with PLA-PEG-(OCH_3) and fluorescently tagged nanoparticles were synthesized. These nanoparticles were delivered to the neuroblastoma cells and uptake was measured by imaging the cells using IVIS after individual incubation periods of 1, 24, 48 and 72-hours

4.2 Materials

For the synthesis of PLA-PEG-(OCH_3), D,L lactide ($C_6H_8O_4$, PURASORB DL) was supplied by Purac Biomaterials. Tin (II) 2-ethylhexanoate ($[CH_3(CH_2)_3CH(C_2H_5)CO_2]_2$- -Sn, ~95%), sodium sulfate (Na_2SO_4,, >99%), anhydrous magnesium sulfate ($MgSO_4$, >99.5%), anhydrous toluene ($C_6H_5CH_3$, 99.8%), methanol (CH_3OH, >99.9%), and chloroform ($CHCl_3$, >99.8%) were supplied by Sigma-Aldrich. Methoxy-poly(ethylene glycol) was supplied by JenKem Technology USA (M-PEG-OH, Mw 5000).

Acetonitrile (C_2H_3N, 99.9%) was supplied by Fisher Scientific. PrestoBlue Cell Viability Reagent and Alexa Fluor 647 cadaverine, were supplied by Life Technologies. For the filtration of the nanoparticles, Molecular weight cutoff centrifugal filter units were purchased from Millipore. Temozolomide was provided by Molekula and O^6-Benzylguanine was provided by Abcam Technologies. 96-well plates, T-75 and T-25 flasks were supplied by GBO.

4.3 Statistical Analysis

All statistical analysis was performed using a two-tailed t-test with at least five repeats each. Statistical significance was set at $p < 0.05$. Error bars on graphs represent the standard deviation from the mean.

4.4. Experiment Methods

4.4.1. Cell Culture

Daoy neuroblastoma cells (American Type Culture Collection, ATCC), D283 neuroblastoma cells (ATCC), SMS-KCNR neuroblastoma cells (ATCC), and SK-N-BE(2) neuroblastoma cells (ATCC) were used for studies. All cells were of human origin and were grown in monolayer cultures at 37°C at 5% of CO_2. Daoy and D283 neuroblastoma cells were cultured using Eagle's Minimum Essential Media (ATCC) supplemented with 10% fetal bovine serum (Atlanta Biologics) and 1% penicillin-streptomycin amphotericin (MediaTech, Inc.) SMS-KCNR cells were cultured using RPMI-1640 Media (ATCC) supplemented with 10% fetal bovine serum and 1% penicillin-streptomycin-amphotericin. SK-N-BE(2) cells were cultured using EMEM/F-12K Media supplemented with 10% fetal bovine serum and 1% penicillin-streptomycin-amphotericin. Cells were passaged and maintained in 75 cm^2 flasks.

4.4.2. Nanoparticle Synthesis & Characterization

Poly(lactide)-poly(ethylene glycol) block copolymers were synthesized with ring-opening polymerization. D,L lactide (17.4 mmol) and methoxy-poly(ethylene glycol)-hydroxyl (0.133 mmol) were placed in a round-bottom flask with sodium sulfate (2.19 mmol) and dried overnight under vacuum (32 in Hg). Reaction components were

dissolved in 10 mL anhydrous toluene at 120°C purged under N_2. Stannous octoate (0.016 mmol) was added to the solution, purged under N_2. The solution was stirred for 12 hours. Next, the reaction vessel was removed from heat and allowed to come to room temperature. The reaction product was washed with chloroform and water in a separation funnel and the bottom phase of the product was collected. Product was dried with magnesium sulfate, filtered, and concentrated using a rotary evaporator. Polymer was then precipitated in cold (-80°C) methanol overnight. Product was collected via centrifugation and lyophilization. Polymers were characterized with nuclear magnetic resonance spectroscopy (Bruker 300 MHz).

Polymeric nanoparticles (NP) were formed using a solvent evaporation technique. PLA-PEG-OCH_3 block copolymer was dissolved in acetonitrile at 5 mg/mL. NPs were synthesized by mixing the polymer solution at a 1:2 ratio in water and stirring for 2 hours. Solutions were collected and washed in 100 kD nominal molecular weight limit (NMWL) centrifugal filter units (3,500 rpm, 7 minutes) twice with water and once with phosphate buffered saline (PBS). NPs were re-suspended in cell culture media at the desired concentration per application.

To synthesize O^6-BG loaded NPS used for drug delivery studies; O6-BG was dissolved in acetonitrile at 2 mg/mL. Then, PLA-PEG was dissolved in the O6-BG containing acetonitrile at 5 mg/mL and allowed to mix on a rotisserie for 1 hour. Nanoparticles were prepared from this solution using the same solvent evaporation technique described previously.

To synthesize fluorescently labeled NPs used in cellular uptake studies, PLA polymer was conjugated with AlexaFluor 647 cadaverine using EDC chemistry. PLA was dissolved in anhydrous dimethylformamide (DMF) and mixed with 10-fold excess EDC. Solution was vortexed and 10-fold excess of AlexaFluor 647 cadaverine was added to the PLA and stirred overnight. This solution was concentrated with the rotary evaporator, re-dissolved in chloroform, precipitated in cold methanol (-80°C), and collected via lyophilization. The final PLA-AF647 polymer was mixed with PLA-PEG in acetonitrile at a 6:4 (PLA-PEG:PLA-647) ratio and NPs were formed using the same solvent evaporation technique described previously.

4.4.3. Free Drug Toxicity for Drug Delivery

To analyze *in vitro* toxicity, D283, Daoy, SK-N-BE(2) and SMS-KCNR neuroblastoma cells were seeded in wells of a black, clear bottom, cell bind 96-well plate at a density of 50,000 cells/well in 200 microliters of cell media. Plates were incubated overnight at 37°C and 5% CO_2 to allow the cells to adhere.

To test free TMZ toxicity, the following day, 1 milligram of TMZ was weighed out and dissolved in 1 milliliter of cell media. Solutions were made at concentrations of 250, 400, 600, 800 and 1000 microgram TMZ/milliliter cell media in a sterile hood. Then, 200 microliters of each drug concentration was added to each of 5 wells with neuroblastoma cells; a control column containing 5 wells of only cell media was also added. 3 well plates were prepared for incubation periods of 24, 48 and 72-hours at 37°C and 5% CO_2. After each respective incubation period, the drug solutions were removed from each well and replaced with 200 microliters of fresh media. After the final

incubation of 72-hours, the cell media was removed and 200 microliters of a 10:1 solution of cell media to Presto Blue Cell Viability Reagent was added to each well. The well plate was then incubated at 37°C and 5% CO_2 for 40 minutes covered from light. The fluorescence signal was then read using a Biotek Synergy 4 fluorescent plate reader with Gen5 1.11 software with an excitation wavelength of 560 nanometers and an emission wavelength of 590 nanometers. The data was then analyzed by comparing the average fluorescent intensity of the samples with 0 microgram/milliliter drug concentration (control) as 100% viability to the average intensity of samples incubated with the various drug concentrations.

To test free O^6-BG toxicity, the day after seeding 96-well plates with cells, 1 milligram of O^6-Benzylguanine was weighed out and dissolved in 100 microliters of Dimethyl Sulfoxide and 1 mL of cell media. Solutions were made at concentrations of 0, 3.125, 6.25, 12.5 and 50 microgram O^6-BG/milliliter of cell media in a sterile hood. Then, 200 microliters of each drug concentration was added to each of 5 wells with neuroblastoma cells; a control column containing 5 wells of only cell media was also added. 3 well plates were prepared for incubation periods of 24, 48 and 72-hours at 37°C and 5% CO_2. After each respective incubation period, the drug solutions were removed from each well and replaced with 200 microliters of fresh media. After the final incubation of 72-hours, the cell media was removed and 200 microliters of a 10:1 solution of cell media to Presto Blue Cell Viability Reagent was added to each well. The well plate was then incubated at 37°C and 5% CO_2 for 40 minutes covered from light. The fluorescence signal was then read using a Biotek Synergy 4 fluorescent plate reader

with Gen5 1.11 software with an excitation wavelength of 560 nanometers and an emission wavelength of 590 nanometers. The data was then analyzed by comparing the average fluorescent intensity of the samples with 0 microgram/milliliter drug concentration (control) as 100% viability to the average intensity of samples incubated with the various drug concentrations.

To test the toxicity of the two drugs in combination, 3 different combination studies were conducted. First, TMZ concentrations were held constant at 128uM and 256uM and O^6-BG was varied at 10, 20, 30 and 64uM; second, O^6-BG concentrations were held constant determined by the results of the free O^6-BG study, while TMZ was varied at 250, 400, 600, 800 and 1000 microgram TMZ/milliliter cell media. To carry out these experiments, cells were seeded in 96-well plates as described previously. The next day, the drugs were weighed out and solutions of the different concentrations were prepared as described previously. Then, 100 microliters of the TMZ solution and 100 microliters of the O^6-BG solution were added to 5 wells of each concentration. A control column of 5 wells containing only cell media and a column of 5 wells containing only the drug administered at constant concentration was also added. 3 well plates were prepared for incubation periods of 24, 48 and 72 hours at 37°C and 5% CO_2. After each respective incubation period, the drug solutions were removed from each well and replaced with 200 microliters of fresh media. After the final incubation of 72-hours, the cell media was removed and 200 microliters of a 10:1 solution of cell media to Presto Blue Cell Viability Reagent was added to each well. The well plate was then incubated at 37°C and 5% CO_2 for 40 minutes covered from light. The fluorescence signal was then read using a Biotek

Synergy 4 fluorescent plate reader with Gen5 1.11 software with an excitation wavelength of 560 nanometers and an emission wavelength of 590 nanometers. The data was then analyzed by comparing the average fluorescent intensity of the samples with 0 microgram/milliliter drug concentration (control) as 100% viability to the average intensity of samples incubated with the various drug concentrations.

4.4.4. O^6-BG Loaded NP & Unloaded NP Toxicity for Drug Delivery

To confirm that O^6-BG and the PLA-PEG-(OCH_3) NP were non-toxic to the neuroblastoma cells, the cells were treated with NP loaded with O^6-BG and unloaded NP. The neuroblastoma cells were seeded in 30 wells of black, clear bottom, cell bind 96-well plates at a density of 50,000 cells/well in 200 microliters of cell media. Plates were then incubated overnight at 37C and 5% CO_2 to allow the cells to adhere. The next day, O^6-BG was encapsulated in NPs using the same solvent evaporation and washing methods described previously, and unloaded NP were prepared the same way. The nanoparticle solutions were prepared at 0.1, 0.5, 1, 2.5, and 5 milligram mPLA-PEG/milliliter cell media in a sterile hood. Then, 200 microliters of each nanoparticle concentration was added to each of 5 wells with neuroblastoma cells. A control column was also added with 5 wells containing only cell media. Plates were prepared based on loaded NP treatment and unloaded NP treatment. 4 plates of each treatment type were made for incubation periods of 12, 24, 48, and 72-hours. The well plates were then incubated at 37C and 5% CO_2. After each incubation period, the cell media containing nanoparticles was removed and 200 microliters of fresh media was added to each well. After the final incubation, the cell media was removed and 200 microliters of a 10:1 solution of cell

media to Presto Blue Cell Viability Reagent was added to each well. The well plate was then incubated at 37C and 5% CO_2 for 40 minutes covered from light. Then, the fluorescence signal was read using a 48Biotek Synergy 4 fluorescent plate reader with Gen5 1.11 software with an excitation wavelength of 560 nanometers and an emission wavelength of 590 nanometers. The data was then analyzed by comparing the average fluorescent intensity of the samples with 0 milligram/milliliter nanoparticle concentration as 100% viability to the average intensity of samples incubated with nanoparticles.

4.4.5. Toxicity of O^6-BG Loaded NP & Free TMZ

To test the effect of combination treatment with O6-BG loaded NP (NPO6) and free TMZ on neuroblastoma cell viability, neuroblastoma cells were seeded in 30 wells of a black, clear bottom, cell bind 96-well plate at a density of 50,000 cells/well in 200 microliters of cell media. Plates were incubated at 37C and 5% CO_2 to allow the cells to adhere. The next day, NPO6 were synthesized using the same encapsulation and solvent evaporation method described previously. Concentration of NP used was the ideal non-toxic concentration determined by the O^6-BG loaded NP studies and O^6-BG concentration was prepared at 2 mg/mL. 1 milligram of TMZ was weighed out and solutions were made at concentrations of 100, 250, 400, and 600 microgram TMZ/milliliter cell media. Then, 100 microliters of the NPO6 solution and 100 microliters of the TMZ solution was added to each of 5 wells per concentration of TMZ. A control column of 5 wells containing only media, and a column containing 5 wells of only NPO6 was also added. After 72 hours, the cell media containing nanoparticles was removed and 200 microliters of a 10:1 solution of cell media to Presto Blue Cell Viability

Reagent was added to each well. The well plate was then incubated at 37C and 5% CO_2 for 40 minutes covered from light. The fluorescence signal was then read using a Biotek Synergy 4 fluorescent plate reader with Gen5 1.11 software with an excitation wavelength of 560 nanometers and emission wavelength of 590 nanometers. The data was then analyzed by comparing the average fluorescent intensity of the samples with 0 microgram/milliliter nanoparticle concentration as 100% viability to the average intensity of samples incubated with TMZ and NPO6.

4.4.6 Quantification of Nanoparticle Uptake into Cells

To analyze nanoparticle uptake into cells, neuroblastoma cells were seeded in 25 wells of a black, clear bottom, cell bind 96-well plate at a density of 50,000 cells/well in 200 microliters of cell media. Plates were incubated at 37C and 5% of CO2 to allow cells to adhere. The next day, AlexaFluor 647 Fluorescently-labeled NPs were synthesized using the method described previously. Then, 200 microliters of the NP at 2 milligrams/milliliter of cell media were added to the wells. 5 columns of 5 wells each were made on the well plate; 1 control column containing only cell media, and the remaining 4 columns for 4 different incubation periods: 1 hour, 24 hours, 48 hours and 72 hours. After each incubation, NP-containing media was removed and wells were gently washed three-times with sterile PBS. Next, wells were trypsinized, collected via centrifugation, and resuspended in 200 μL sterile PBS. Samples were then transferred to a new 96-well plate, with fluorescent measurements (Ex/Em 645/680) recorded for each sample.

4.5. Experiment Results and Discussion

4.5.1. Synthesis of PLA-PEG-(OCH_3)

Synthesis of PLA-PEG-(OCH_3) polymeric nanoparticles was successful in yielding biocompatible particles for the use in drug delivery applications. Figure 3 shows the particle size profiles of the nanoparticles while Figure 4 shows the particle size profiles of the O^6-BG loaded nanoparticles. To describe the basic nanoparticle structure, PLA is generally hydrophobic and therefore forms the core of the spherical nanoparticle, while the hydrophilic PEG forms the protective outer shell.

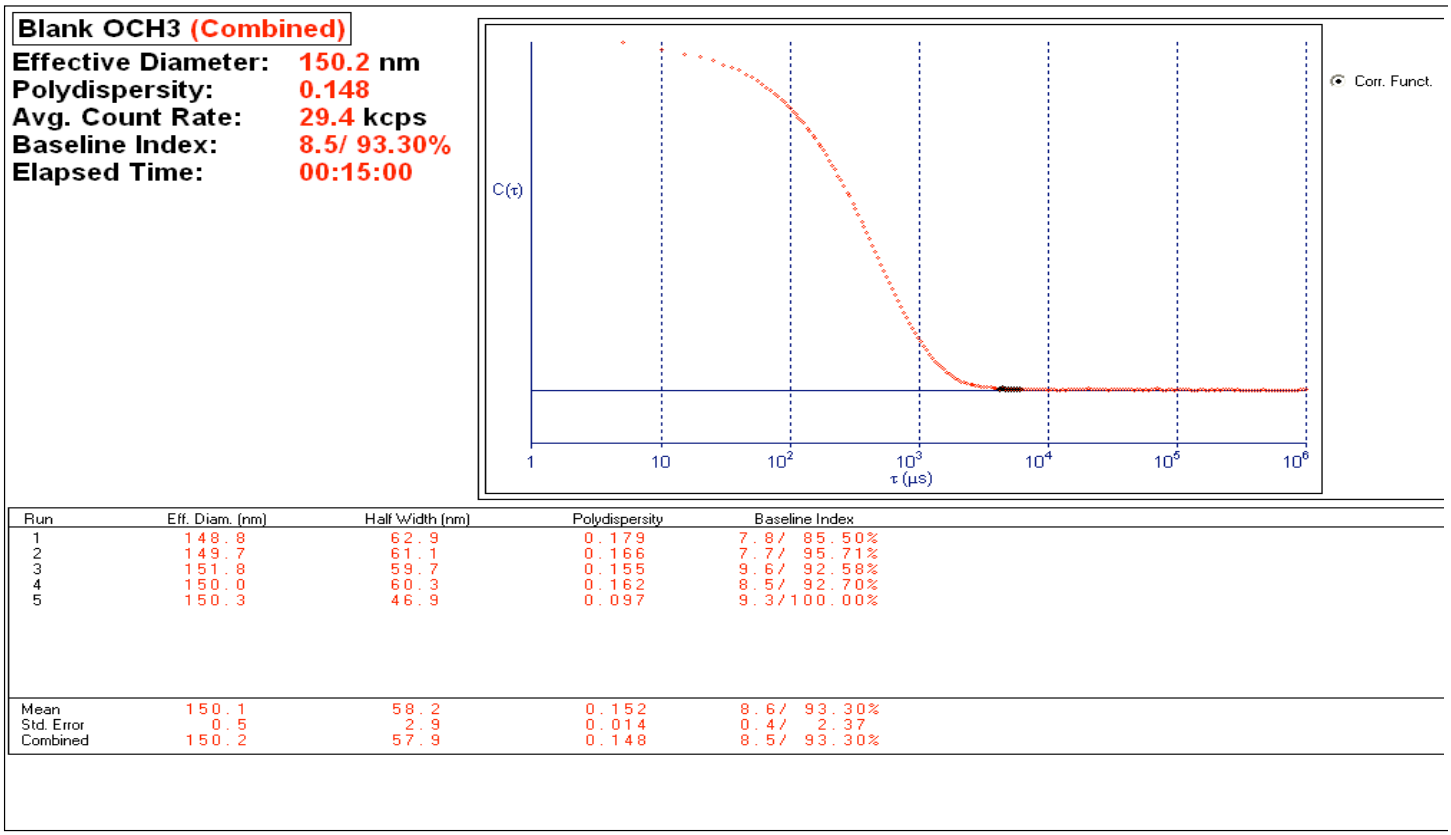

Figure 3 | Particle size distribution of PLA-PEG(OCH_3) nanoparticles. Acquired using BIC Particle Size Software.

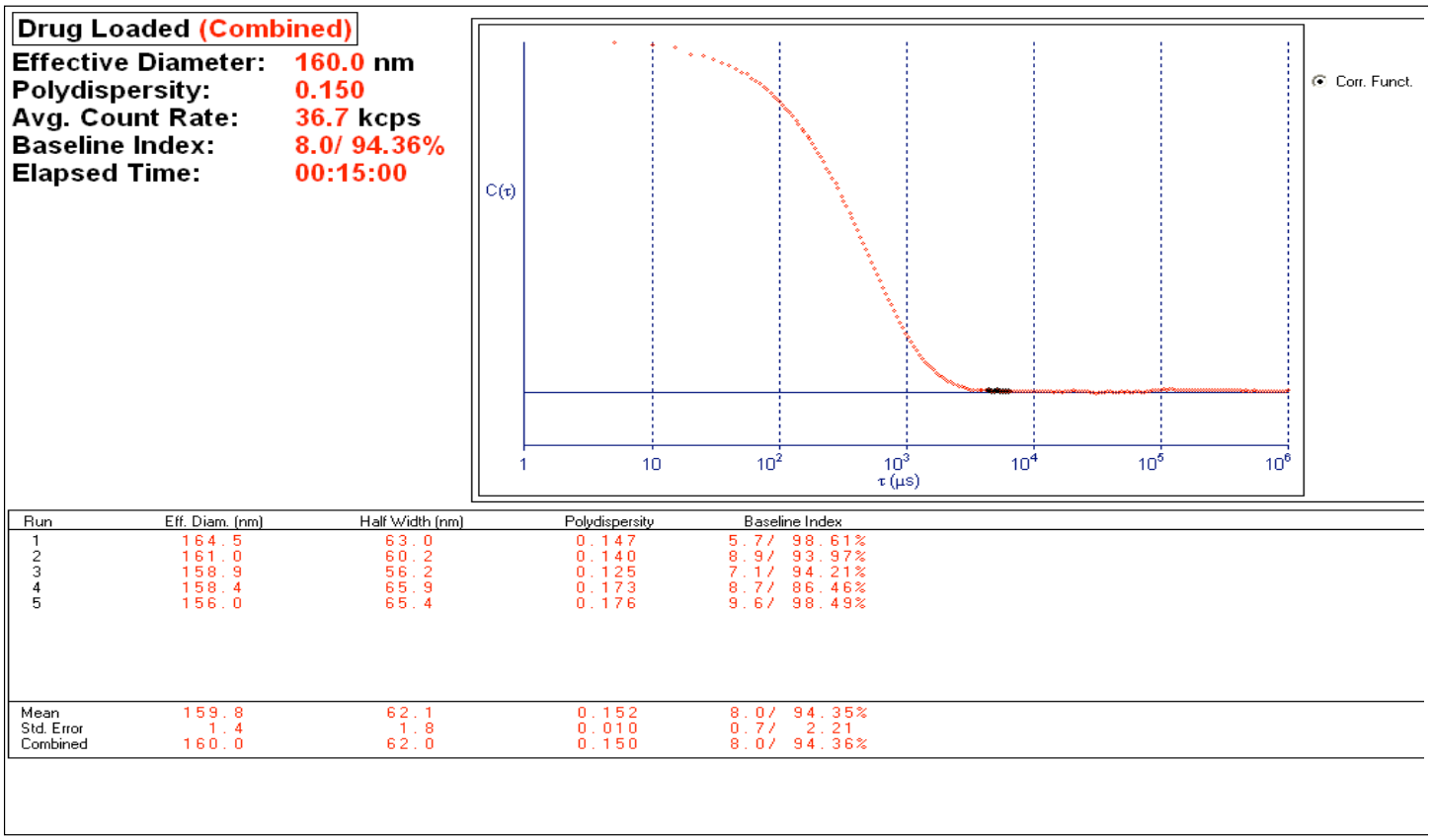

Run	Eff. Diam. (nm)	Half Width (nm)	Polydispersity	Baseline Index
1	164.5	63.0	0.147	5.7/ 98.61%
2	161.0	60.2	0.140	8.9/ 93.97%
3	158.9	56.2	0.125	7.1/ 94.21%
4	158.4	65.9	0.173	8.7/ 86.46%
5	156.0	65.4	0.176	9.6/ 98.49%
Mean	159.8	62.1	0.152	8.0/ 94.35%
Std. Error	1.4	1.8	0.010	0.7/ 2.21
Combined	160.0	62.0	0.150	8.0/ 94.36%

Figure 4 | Particle size distribution of O6-BG loaded PLA-PEG(OCH_3) NP. Acquired using BIC Particle Size Software.

4.5.2. Western Blot Data

Figure 5 below displays the relative amounts of MGMT expression in various neuroblastoma tumor cells. It is important to examine this data to determine the varying MGMT levels in each cell line tested, and to be able to compare which cell lines express the most and the least MGMT. This allows for determination of which cell lines would be expected to show the most and least amount of drug resistance. Figure 6 quantifies the western blot images into relative values of expression. To do this, MGMT to ß-actin ratio was calculated and the values were normalized to DAOY, since it had the lowest MGMT:ß-actin value.

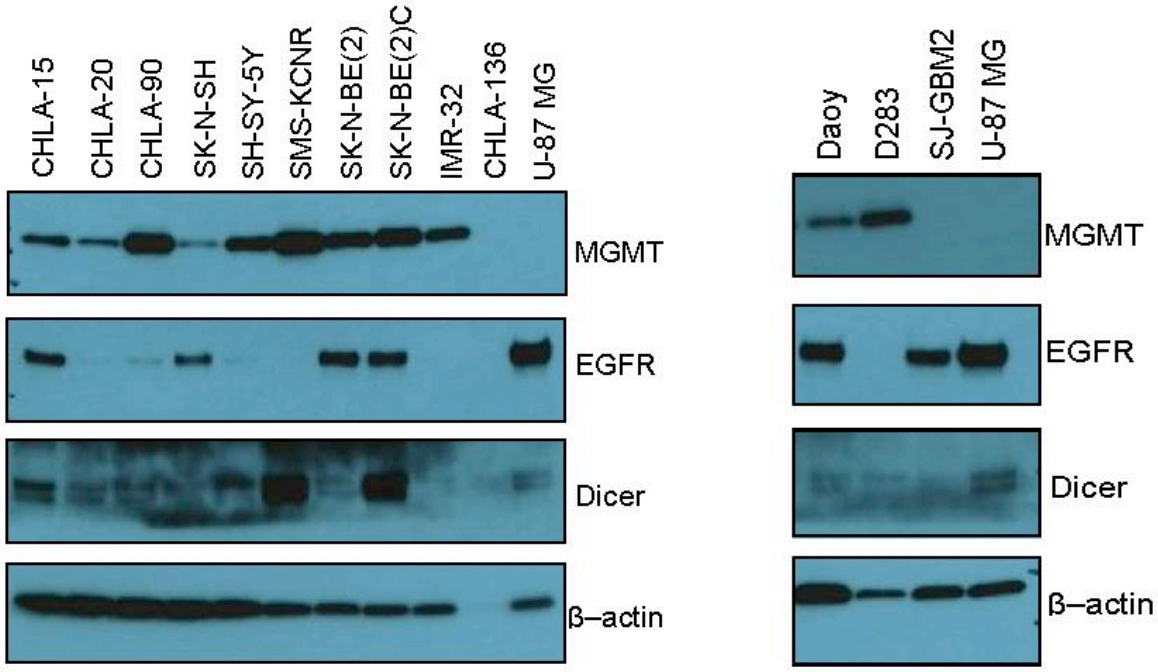

Figure 5 | Western Blot Results showing protein expression in various neuroblastoma and brain tumor cell lines. Credit: Dr. Jacqueline Kraveka, MUSC

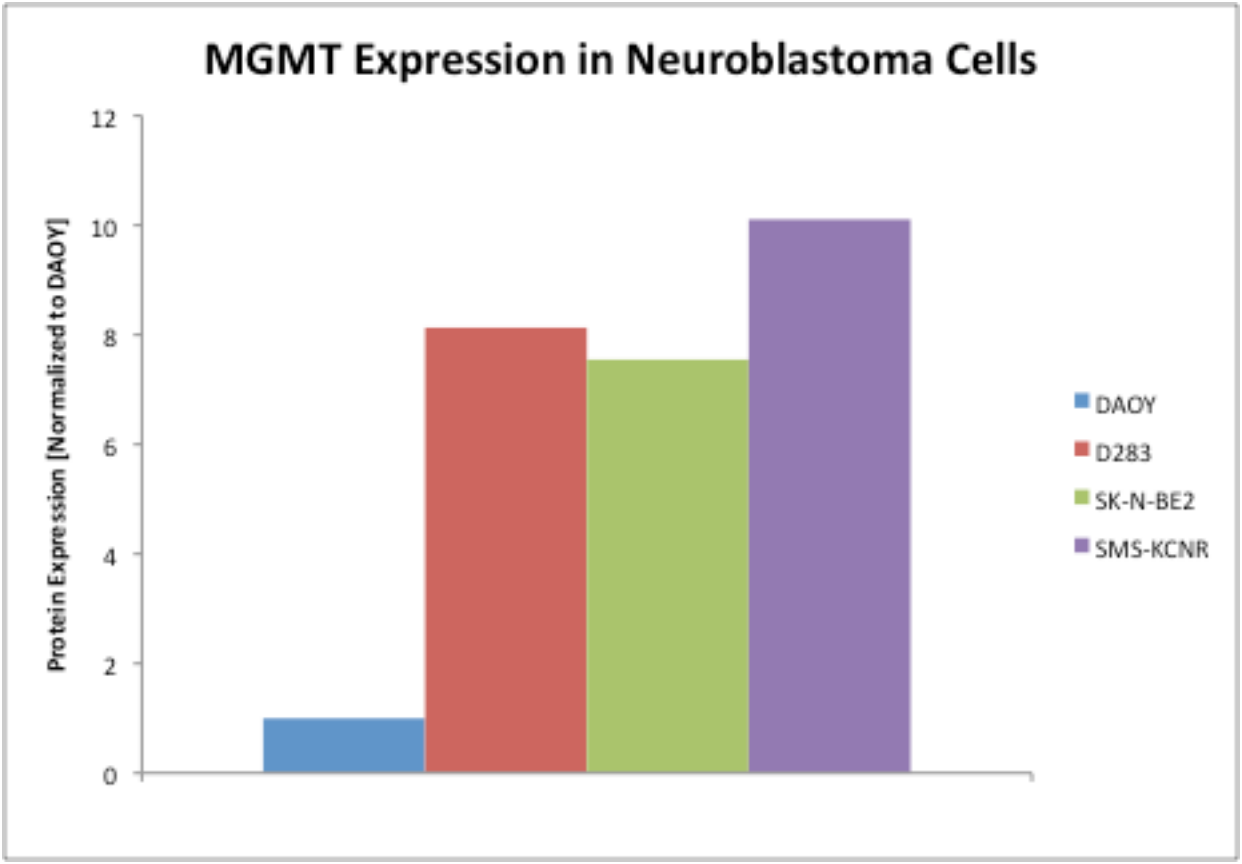

Figure 6 | Graph of MGMT protein expression in each cell line. Values are normalized to β-actin protein.

4.5.3. O^6-BG Toxicity

Toxicity studies were performed to determine the interaction the drug O^6-BG would have with a neuroblastoma cell. This was conducted on the 4 cell lines, Daoy, D-283, SK-N-BE(2), and SMS-KCNR. The results of this study were used to determine the concentration of O^6-BG to be used in TMZ+O6 combination studies. These studies showed minimal toxicity in the cells, since O^6-BG is a non-toxic drug. 80% viability was viewed as an acceptable toxicity level for the purposes of this study.

The viability of D-283 cells remained around 80% even at higher drug concentrations such as 256 µM up to 24 hours incubation, but progressively declined to around 60% as incubation time increased to 72 hours. For this cell line, 64 µM was determined as the concentration of O^6-BG to be used for the drug combination studies.

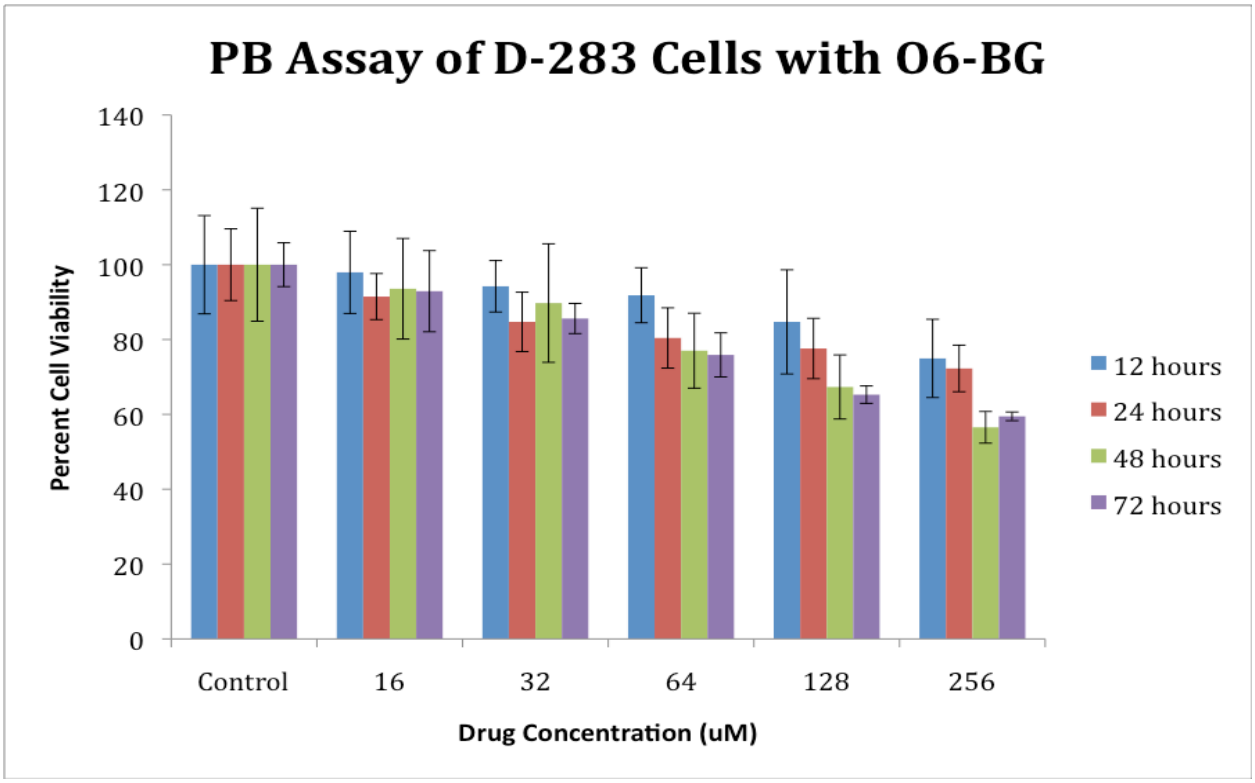

Figure 7 | Toxicity of O^6-BG in D-283 Cells. Cell viability around 80% for elevated drug concentration indicates an acceptable toxicity

In Daoy cells, viability remained around 75-80% even as drug concentration was elevated to 256uM and incubation period was increased to 72 hours. For this cell line, 128 µM was determined as the O^6-BG concentration to be used in the drug combination studies.

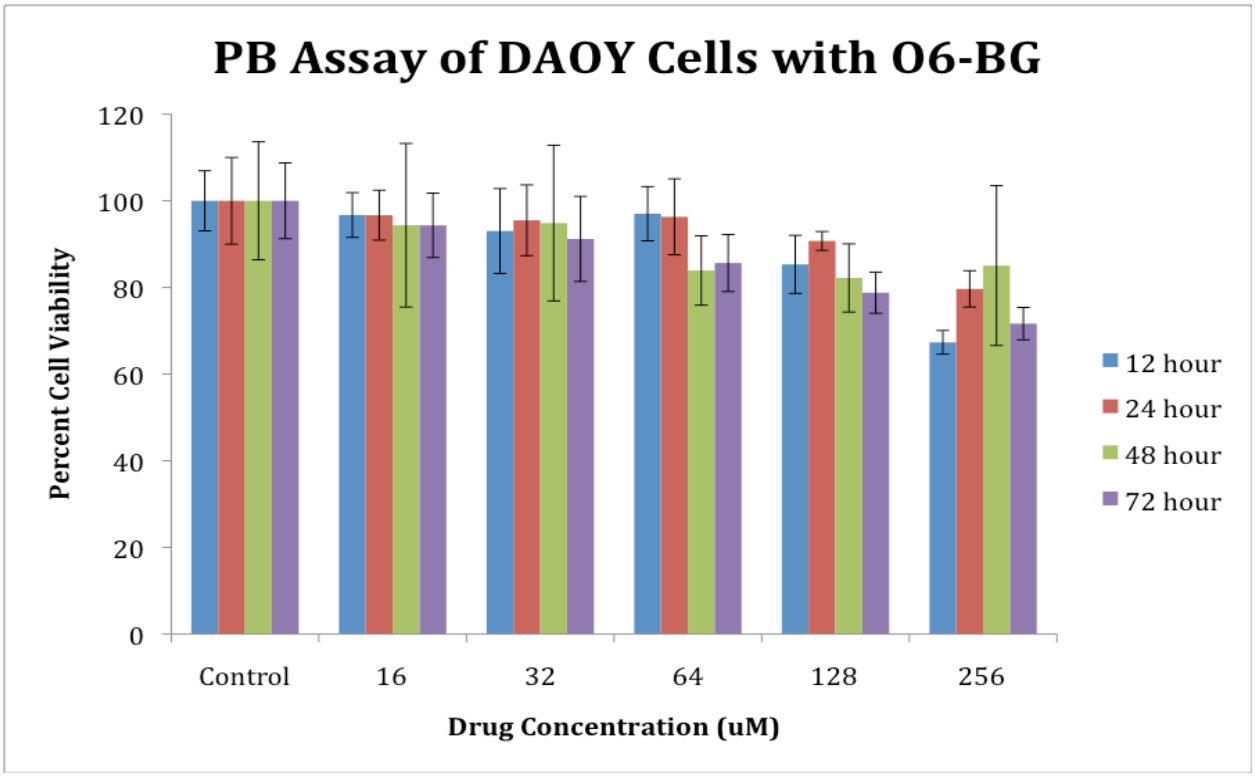

Figure 8 | Toxicity of O^6-BG in Daoy Cells. Cell viability around 80% for elevated drug concentration indicates an acceptable toxicity.

In SK-N-BE(2) cells, there was more variability in cell viability. Viability remained above 80% up to 24 hours at concentrations up to 128 μM, dropped significantly at 48 hours down to almost 40% at 256 μM. At 72 hours, however, viability remained well above 80% up to 256 μM. For this cell line, 64 μM was determined to be the concentration of O^6-BG used in the drug combination studies.

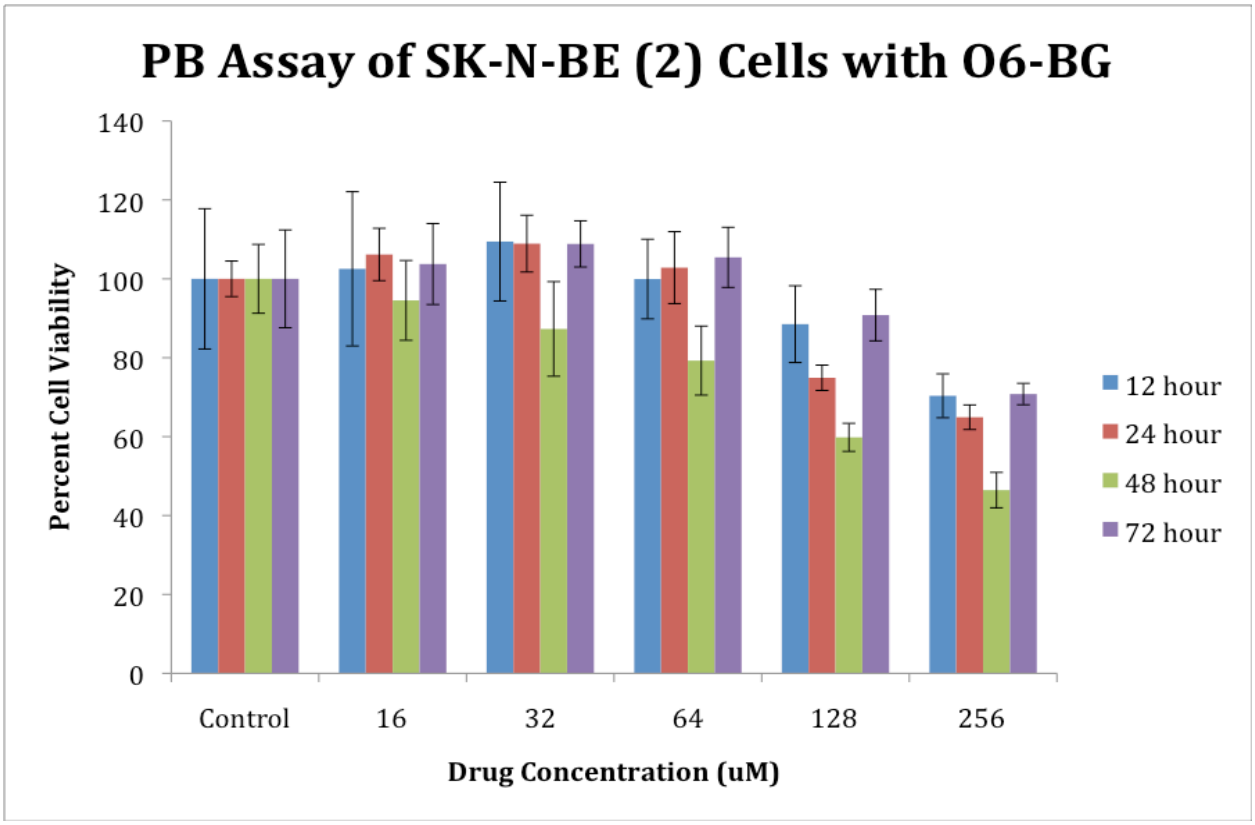

Figure 9 | Toxicity of O^6-BG in SK-N-BE(2) Cells. Cell viability around 80% for elevated drug concentration indicates an acceptable toxicity.

In SMS-KCNR cells, viability remained around or above 80% until 24 hours up to 128 μM, however slightly dropped after 48 and 72 hours to 65-70% viability and decreased to around 60% at the highest conentration of 256 μM. For this cell line, 64 μM was determined to be the concentration of O^6-BG used in the drug combination studies.

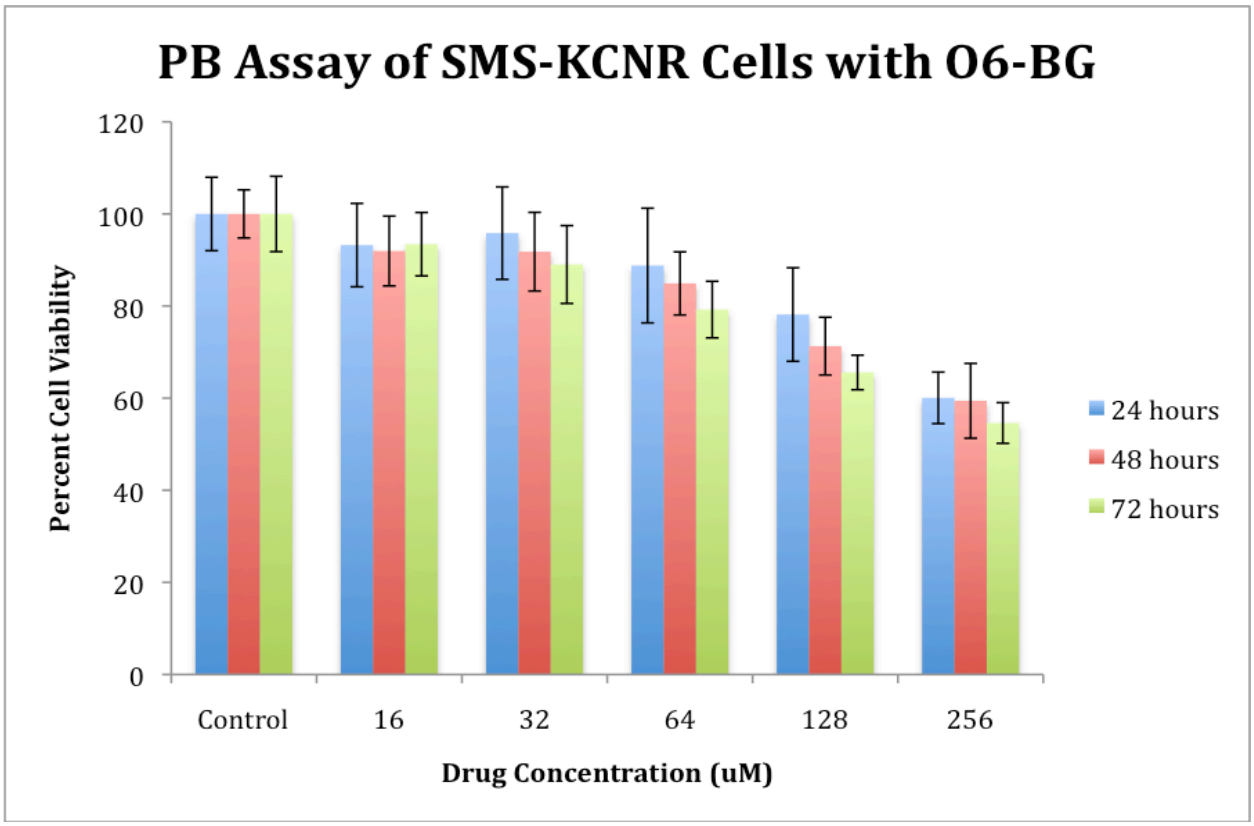

Figure 10 | Toxicity of O^6-BG in SMS-KCNR Cells. Cell viability around 80% for elevated drug concentration indicates an acceptable toxicity.

4.5.4. Nanoparticle Toxicity

Toxicity studies were performed to determine the interaction the PLA-PEG-(OCH_3) particles and the O^6-BG loaded PLA-PEG-(OCH_3) particles would have with the neuroblastoma cells. These studies showed minimal toxicity in the cells. For the purposes of this study, 80% viability was considered to be an acceptable toxicity level. The results of this study were used to determine what concentration of nanoparticles should be used for the NPO6+TMZ combination drug studies.

In D-283 cells, there was no toxicity associated with either the unloaded nanoparticles or the drug-loaded nanoparticles. Cell viability remained close to 100% up

to the highest concentration of 5 mg/mL. For this cell line, 5 mg/mL was determined to be the concentration of nanoparticles used in NPO6+TMZ combination drug studies.

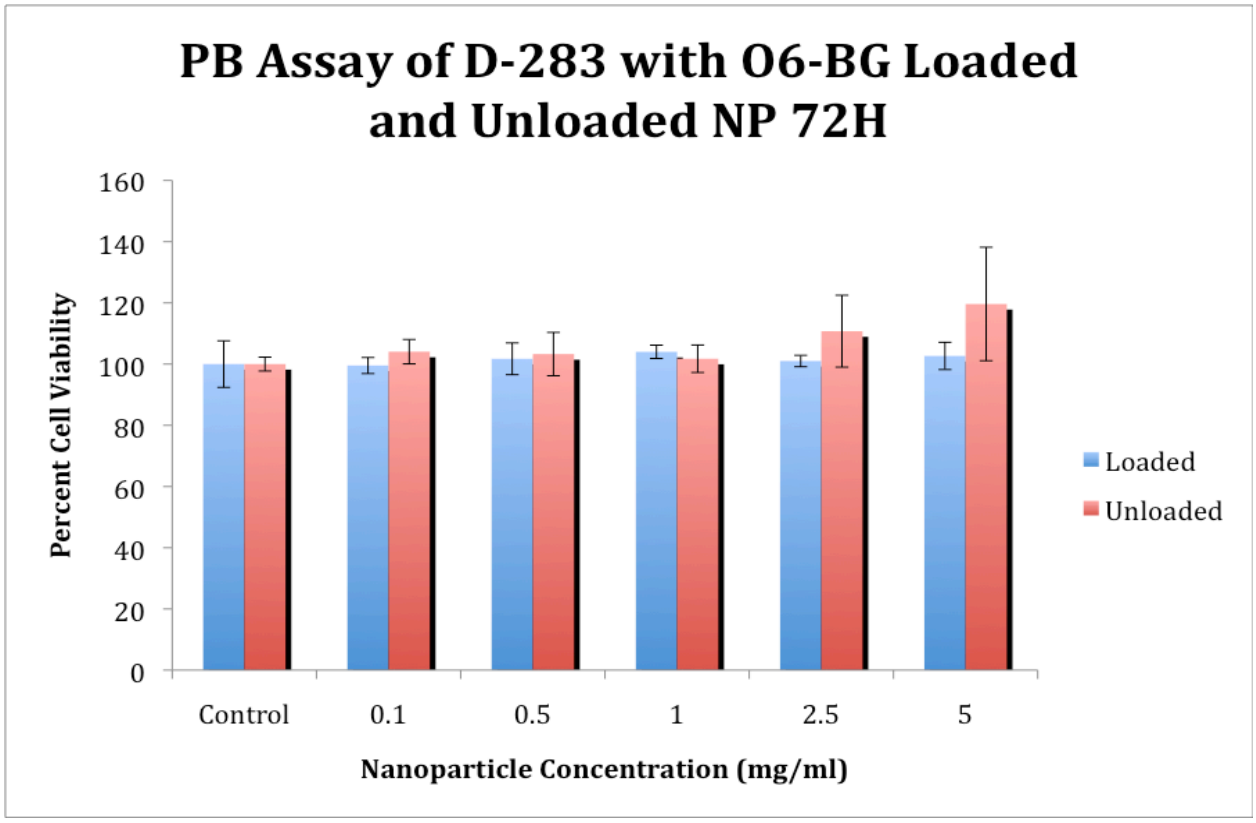

Figure 11 | Toxicity of O^6-BG loaded vs unloaded PLA-PEG-(OCH_3) NP in D-283 Cells. Cell viability around 80% for elevated nanoparticle concentration indicates an acceptable toxicity.

In Daoy cells, there was no toxicity associated with either the unloaded NP or the drug-loaded NP. Cell viability remained close to 100% up to 2.5 mg/ml and declined to around 70% at 5 mg/ml concentration. For this cell line, 2.5 mg/ml was determined to be the concentration used in the NPO6+TMZ drug combination studies.

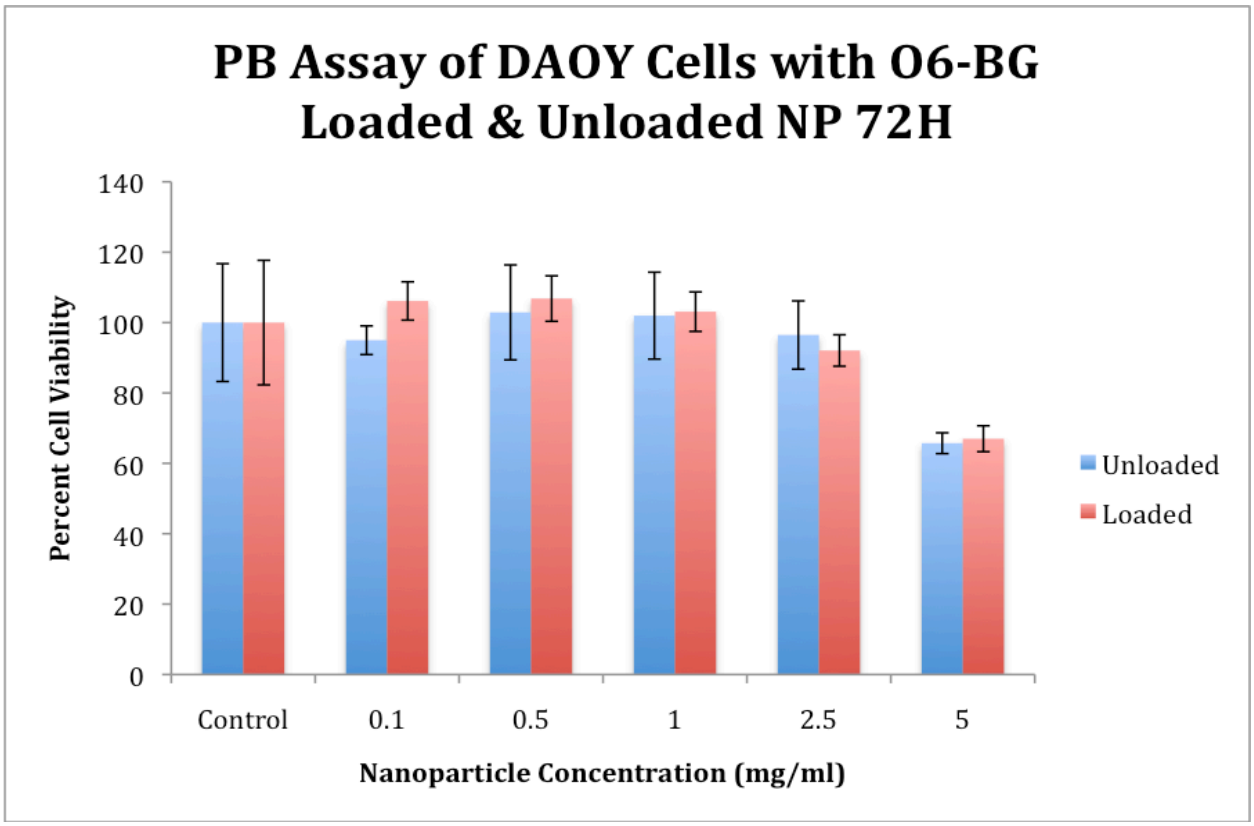

Figure 12 | Toxicity of O^6-BG loaded vs unloaded PLA-PEG-(OCH_3) NP in Daoy Cells. Cell viability around 80% for elevated nanoparticle concentration indicates an acceptable toxicity.

SK-N-BE(2) cells also exhibited no toxicity as a result of both nanoparticle treatments. Viability remained close to 100% for all concentrations and nanoparticle treatments. Only at 1 mg/ml did the cell viability decrease to around 80% with the drug-loaded nanoparticles. For this cell line, 5 mg/ml was determined to be the concentration used for the NPO6+TMZ drug combination studies.

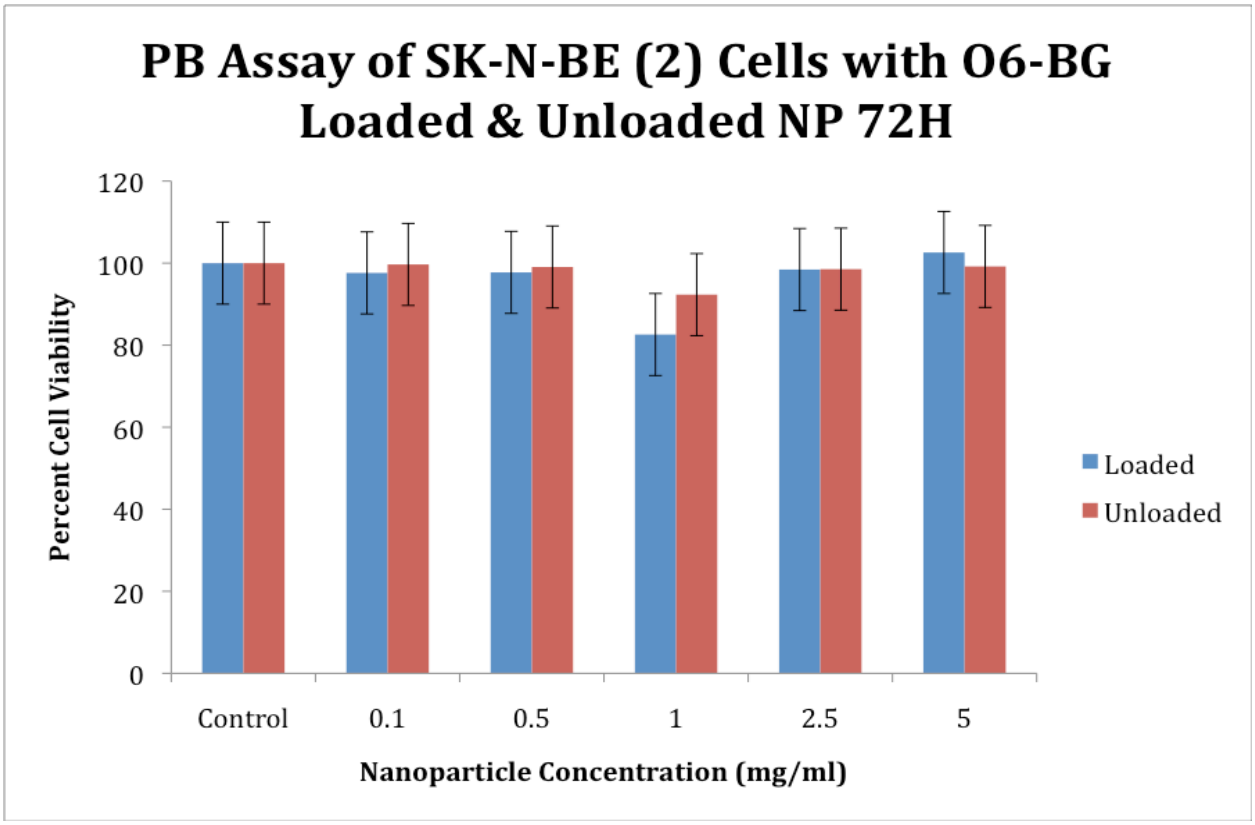

Figure 13 | Toxicity of O^6-BG loaded vs unloaded PLA-PEG-(OCH_3) NP in SK-N-BE(2) Cells. Cell viability around 80% for elevated nanoparticle concentration indicates an acceptable toxicity

In SMS-KCNR cells, there was no toxicity associated with the unloaded nanoparticle treatment and minimal toxicity associated with the loaded-nanoparticle treatment. Cell viability in the loaded-nanoparticle remained around 100% up to 1 mg/ml, and decreased to 80% and 70% at 2.5 and 5 mg/ml, respectively. For this cell line, 2.5 mg/ml was determined to be the concentration used for the NPO6+TMZ drug combination studies.

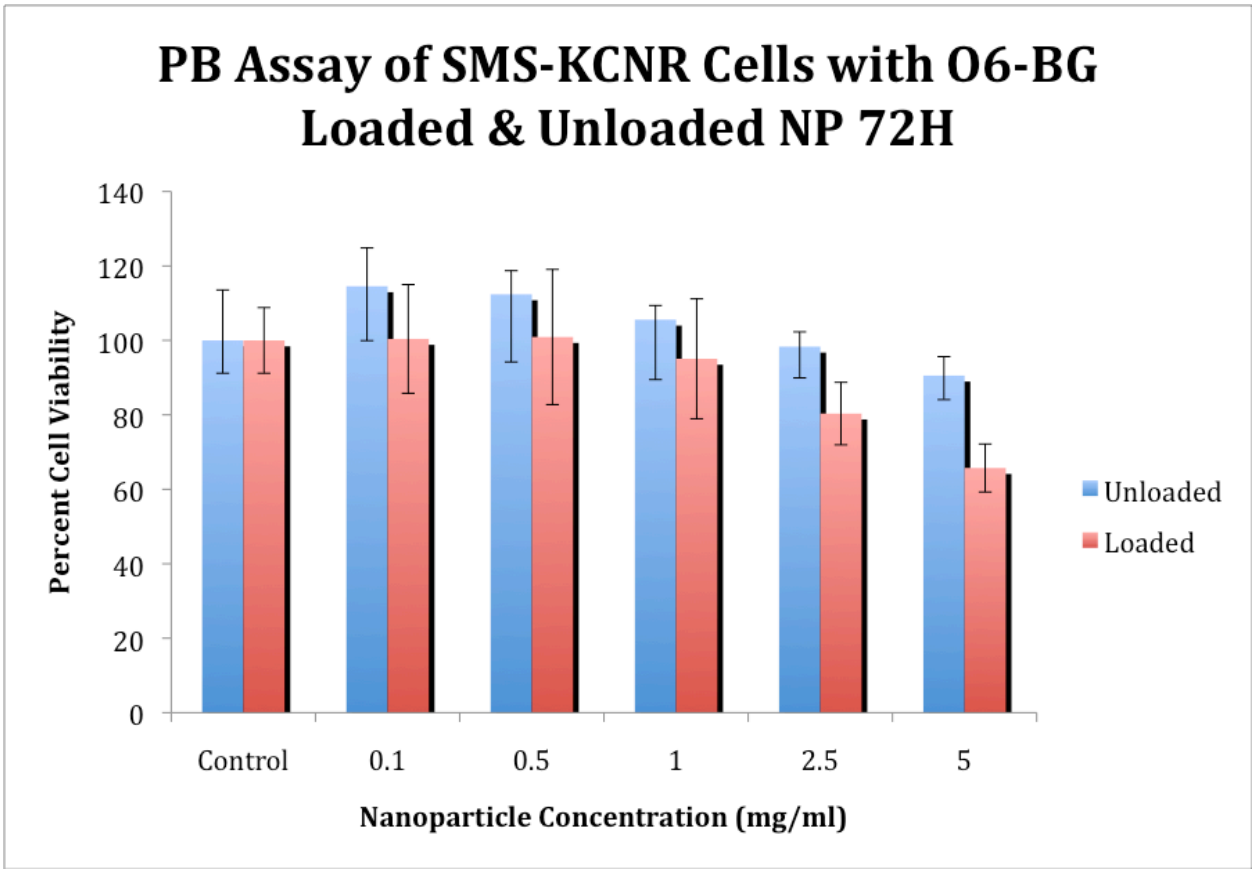

Figure 14 | Toxicity of O^6-BG loaded vs unloaded PLA-PEG-(OCH_3) NP in SMS-KCNR Cells. Cell viability around 80% for elevated nanoparticle concentration indicates an acceptable toxicity.

4.5.5. TMZ Toxicity

Toxicity studies were performed to determine the interaction the drug Temozolomide (TMZ) would have with a neuroblastoma cell. This was conducted on the 4 cell lines, Daoy, D-283, SK-N-BE(2), and SMS-KCNR. The results of this study were used to determine the highest concentration of TMZ that could be administered without causing toxicity to normal cells. TMZ is a toxic drug, so a higher level of toxicity was expected. Viability above 40% was viewed as an acceptable toxicity level for the purposes of this study.

In D-283 cells, viability decreased steadily with increasing TMZ concentration. At these concentrations, it is clear that TMZ had a fairly toxic effect on the cells, especially at 800 and 1000 µg/ml, cell viability remained below 40%, which would likely affect normal cells as well. Cell viability remained above 40% for 250 and 600 µg/ml. Based on this study, TMZ concentrations up to 600 µg/ml were determined to be used for the NPO6+TMZ drug combination studies.

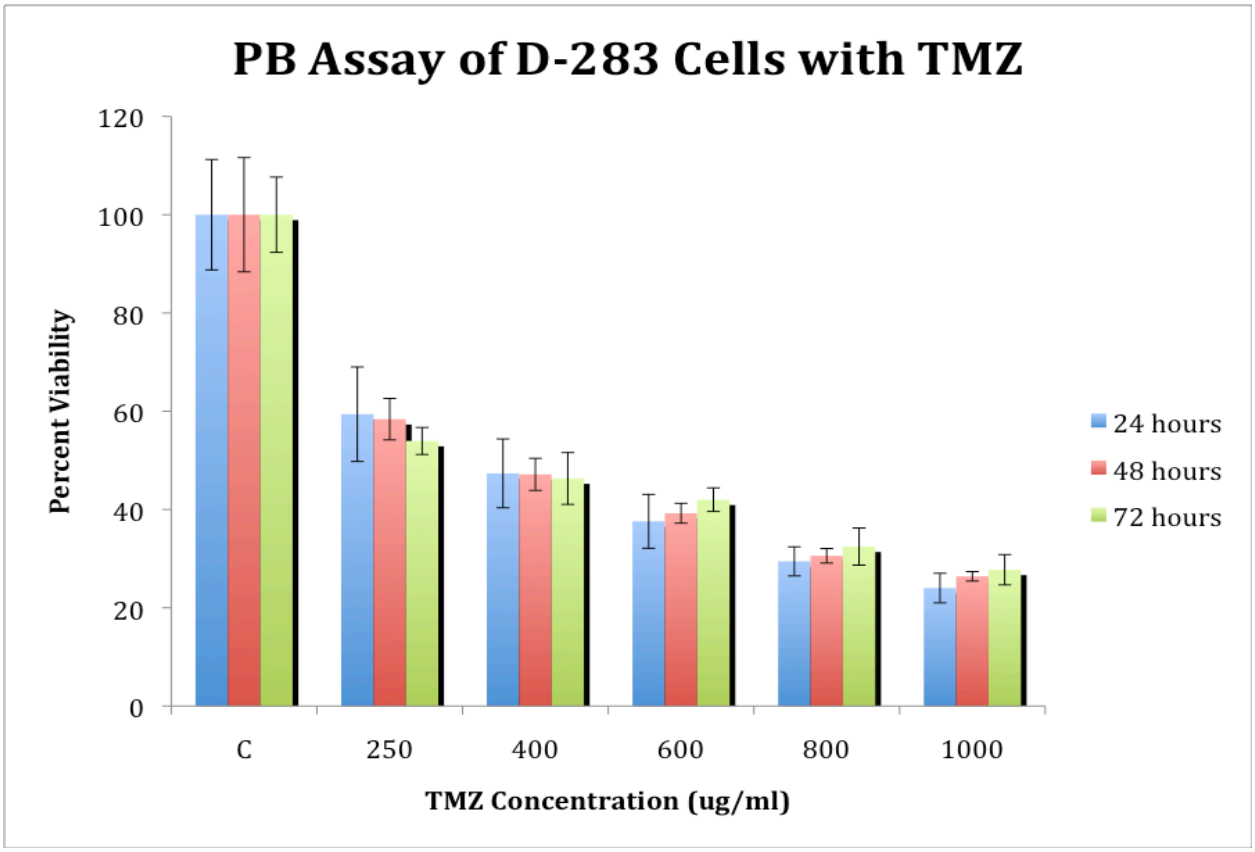

Figure 15 | Toxicity of TMZ in D-283 Cells. Cell viability above 40% for elevated TMZ concentration indicates an acceptable toxicity.

In Daoy cells, there was a dramatic decrease in cell viability with increasing TMZ concentration. Viability remained above 40% for 250 and 400 µg/ml incubation. Post this point, viability dropped below 40% for all higher concentrations up to 1000 µg/ml.

Based on this study, TMZ concentrations up to 600 µg/ml were determined to be the concentrations used for the NPO6+TMZ drug combination studies.

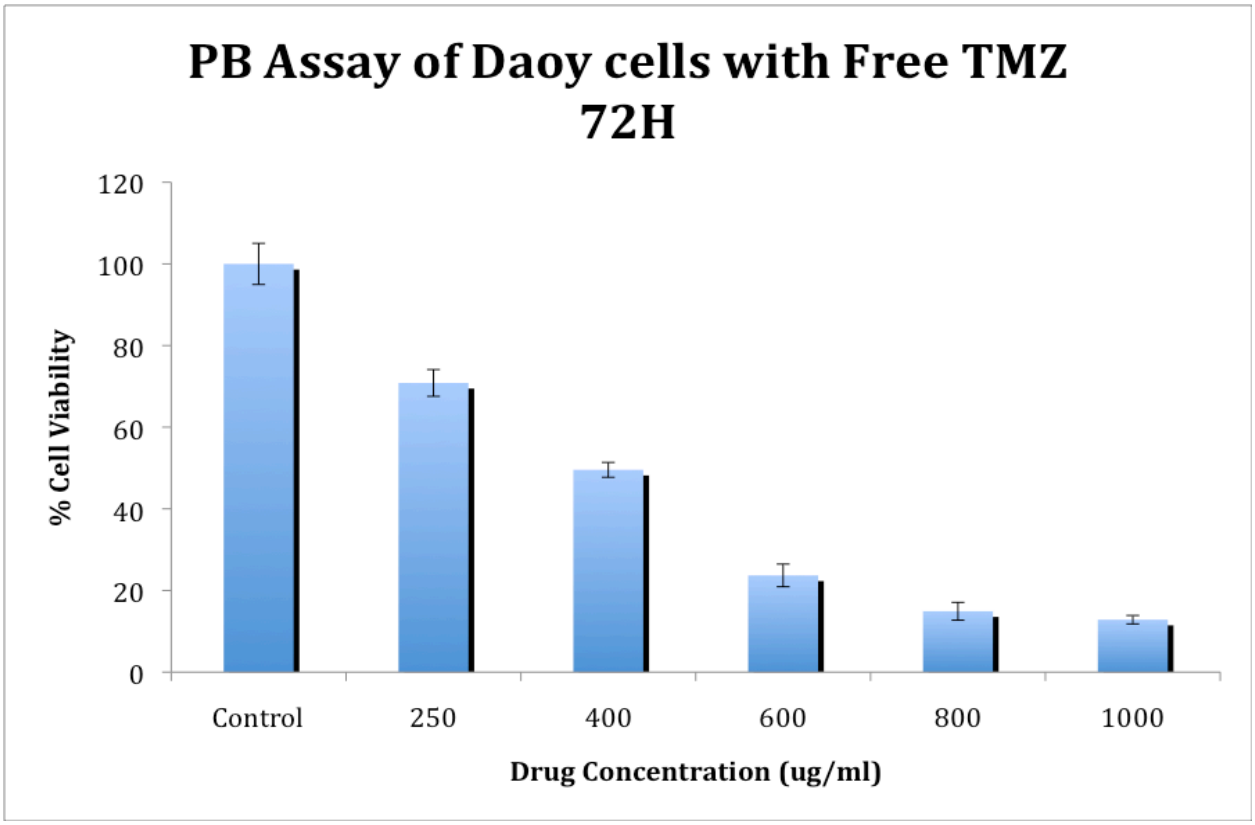

Figure 16 | Toxicity of TMZ in Daoy Cells. Cell viability above 40% for elevated TMZ concentration indicates an acceptable toxicity.

In SK-N-BE(2) cells, viability remained close to 40% up to 400 µg/ml and dropped below 40% from 600-1000 µg/ml. Based on this study, TMZ concentrations of up to 600 µg/ml were used for the NPO6+TMZ drug combination studies.

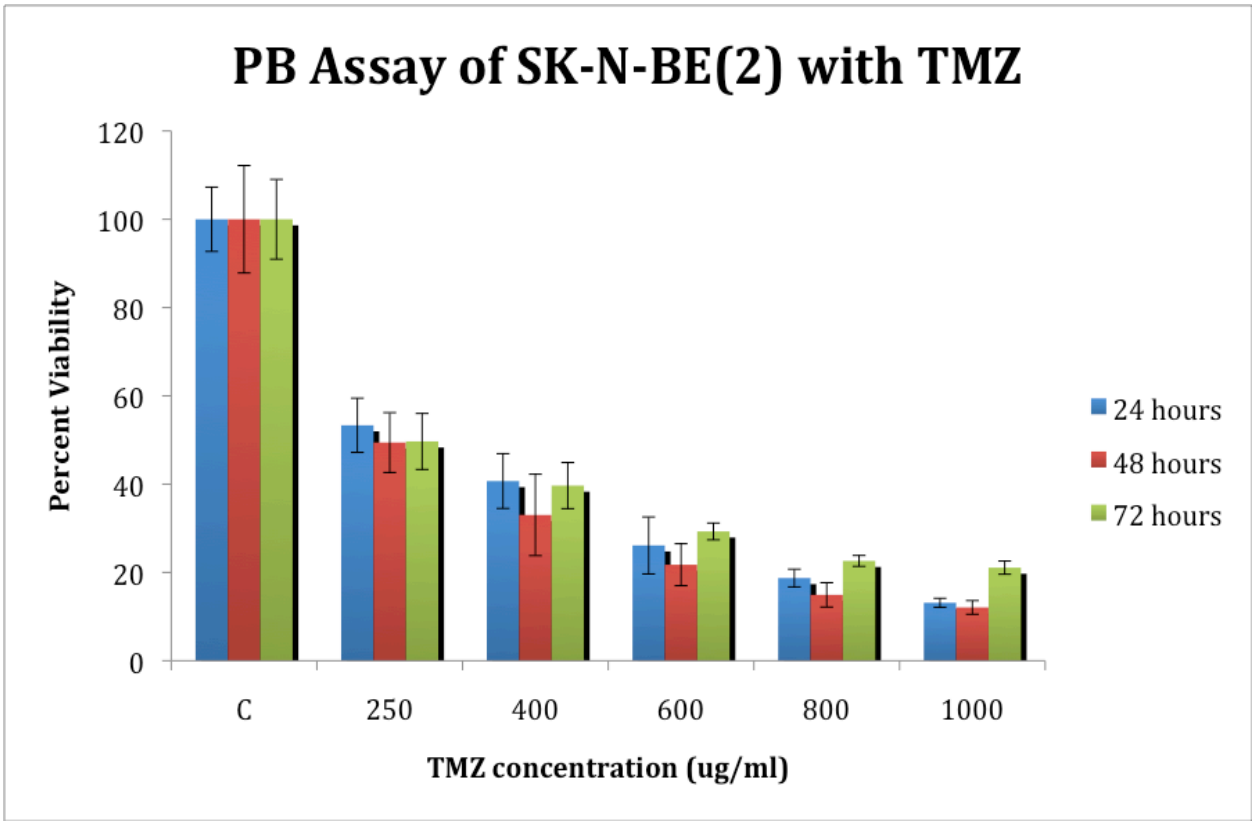

Figure 17 | Toxicity of TMZ in SK-N-BE(2) Cells. Cell viability above 40% for elevated TMZ concentration indicates an acceptable toxicity.

In SMS-KCNR cells, there was a high level of toxicity associated with TMZ. Cell viability remained below 50% for all concentrations of TMZ, and dropped below 40% at 400 µg/ml up to 1000 µg/ml. Based on this study, TMZ concentrations up to 600 µg/ml were used for the NPO6+TMZ drug combination studies.

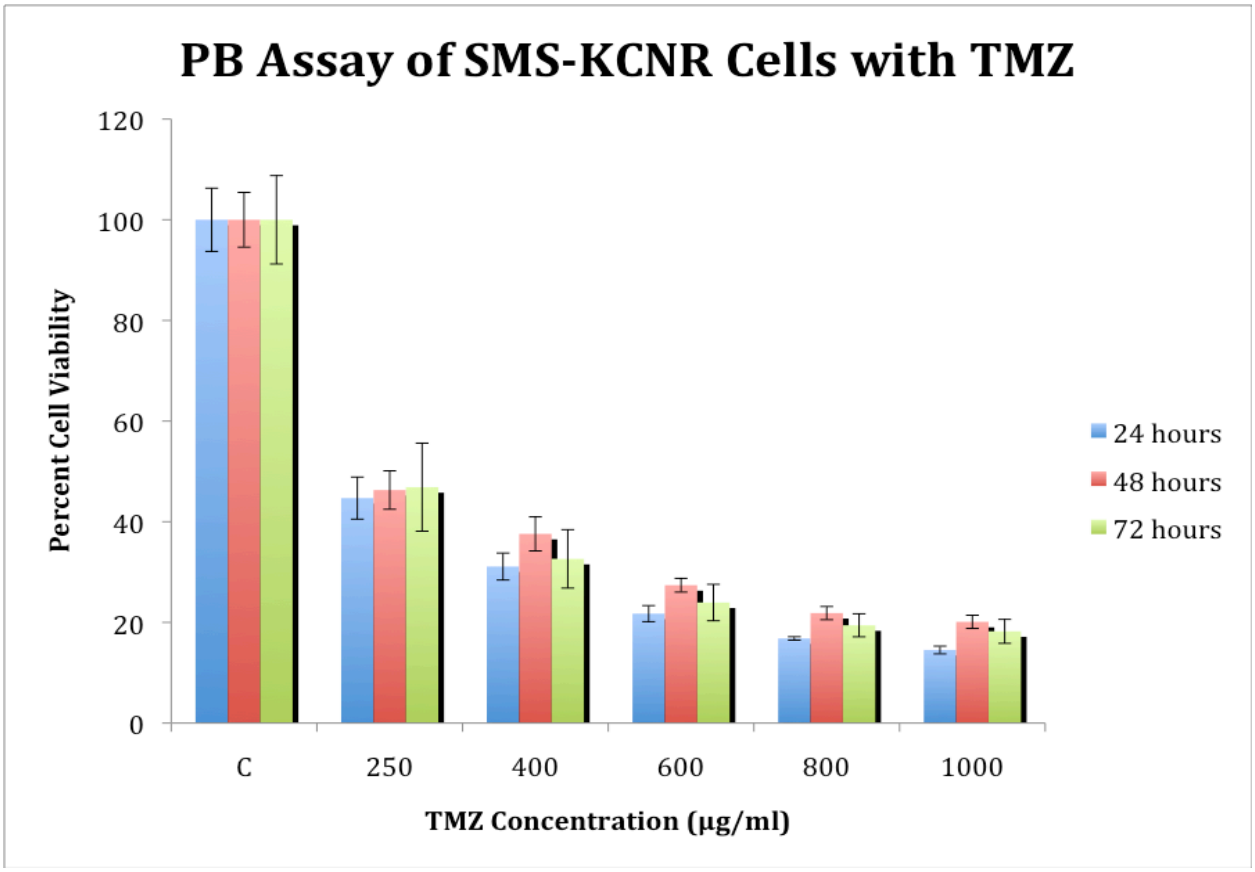

Figure 18 | Toxicity of TMZ in SMS-KCNR Cells. Cell viability above 40% for elevated TMZ concentration indicates an acceptable toxicity.

4.5.6. Free Drug Combination Toxicity

Toxicity studies were performed to determine the interaction both drugs, O^6-BG and TMZ, in combination would have on a neuroblastoma cell. This test was conducted on the 4 cell lines, D-283, Daoy, SK-N-BE(2), and SMS-KCNR. The results of this study were used to determine the effect O^6-BG would have on enhancing TMZ toxicity, as hypothesized. These studies showed a high level of toxicity, as TMZ concentration increased with a constant concentration O^6-BG. Cell viability above 40% was viewed as an acceptable toxicity level for the purposes of this study.

In D-283 cells, there was a high level of toxicity as TMZ concentration increased from 250 µg/ml to 1000 µg/ml. Viability remained 40-60% up to 400 µg/ml and dropped below 40% at 600 µg/ml up to 1000 µg/ml. O^6-BG concentration was held constant at 64 µM which was determined by the results of the free O^6-BG toxicity studies. It was also determined that the concentration of TMZ administered would not exceed 600 µg/ml for the NPO6+TMZ studies.

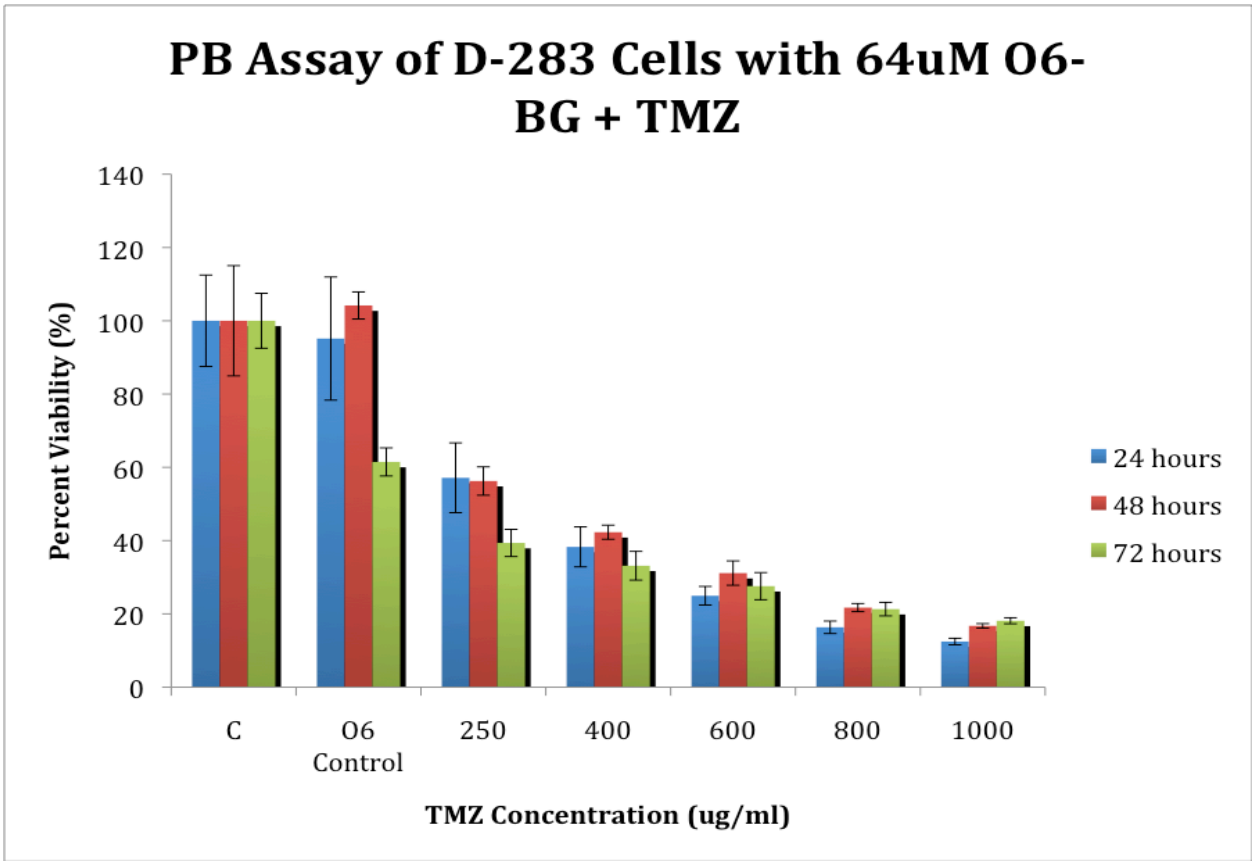

Figure 19 | Toxicity of O^6-BG & TMZ in D-283 Cells. Cell viability above 40% for elevated TMZ concentration indicates an acceptable toxicity.

Figure 20 shows the results of administering 128 µM O^6-BG with increasing concentrations of TMZ after 72 hours incubation. The combination of TMZ and O^6-BG resulted in a high level of toxicity, with cell viability remaining below 40% at concentrations above 250 µg/ml. Based on this study, it was determined that TMZ concentrations up to 600 µg/ml would be used for the NPO6+TMZ drug combination studies.

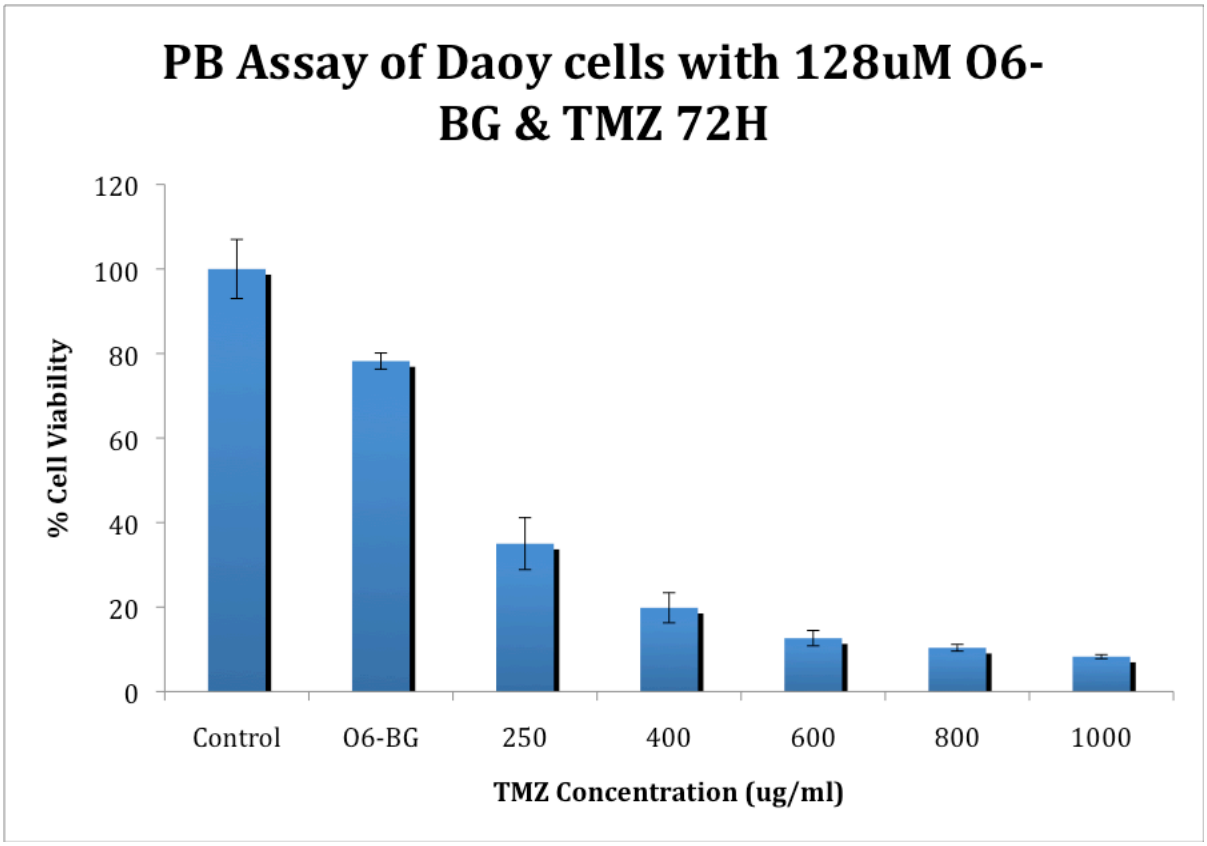

Figure 20 | Toxicity of O^6-BG & TMZ in Daoy Cells at 72H. Cell viability above 40% for elevated TMZ concentration indicates an acceptable toxicity level.

In SK-N-BE(2) cells, viability was high, around 70%, at TMZ concentration of 250 µg/ml and 64 µM O^6-BG. At 400 µg/ml TMZ, viability dropped below 40% and continued to decline up to 1000 µg/ml. For this cell line, it was determined that TMZ concentrations up to 600 µg/ml would be used for the NPO6+TMZ drug combination studies.

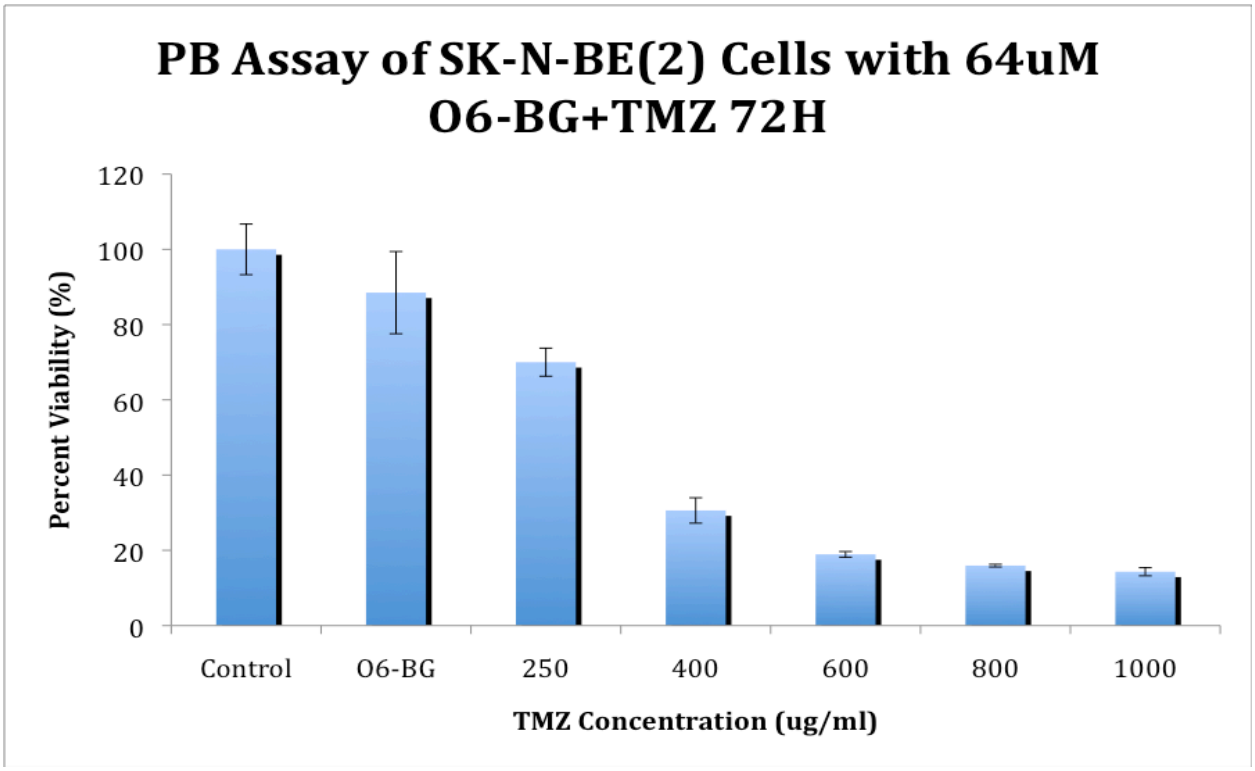

Figure 21 | Toxicity of O^6-BG & TMZ in SK-N-BE(2) Cells at 72H. Cell viability above 40% for elevated TMZ concentration indicates an acceptable toxicity level.

In SMS-KCNR cells, cell viability remained above 40% up to 400 µg/ml TMZ, and dropped below 40% at 600 µg/ml up to 1000 µg/ml after 24 hours incubation. After 48 hours incubation, cell viability dropped below 40% at 400 µg/ml and at 250 µg/ml

after 72 hours incubation. For this cell line, it was determined that TMZ concentrations up to 600 µg/ml would be used for the NPO6+TMZ drug combination studies.

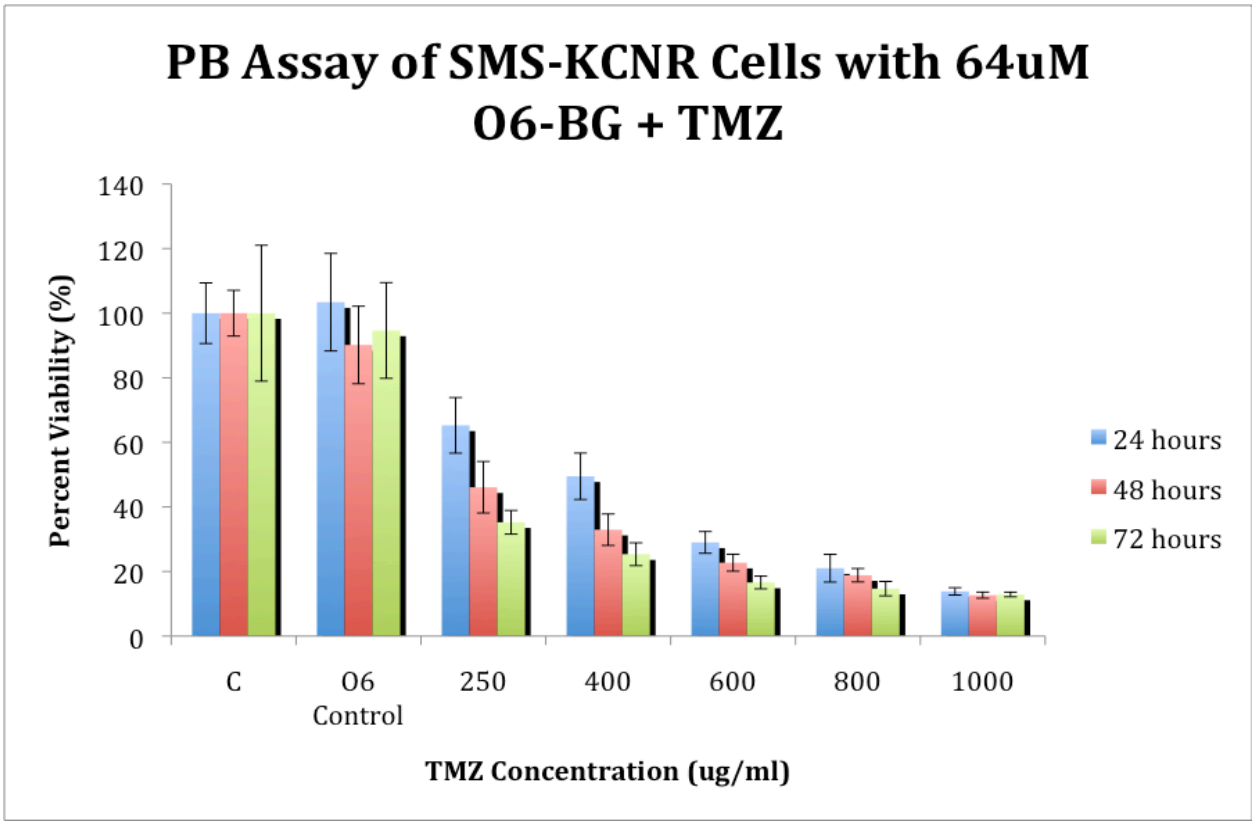

Figure 22 | Toxicity of O^6-BG & TMZ in SMS-KCNR Cells. Cell viability above 40% for elevated TMZ concentration indicates an acceptable toxicity level.

4.5.7. O^6-BG Loaded Nanoparticles with TMZ Toxicity

Toxicity studies were performed to determine the interaction of combining nanoparticles loaded with O^6-BG and free TMZ with neuroblastoma cells. These tests were conducted on the 4 cell lines, D-283, Daoy, SK-N-BE(2), and SMS-KCNR. O^6-BG was loaded at 2 milligrams/milliliter concentration in the nanoparticles and administered with varying TMZ concentrations from 100 to 600 µg/ml. It was expected to observe a

significant level of toxicity, indicating that this combination therapy would enhance the efficacy of TMZ as a therapeutic through the aid of the MGMT-inhibiting properties of O^6-BG. A toxicity level greater that 40% (less than 60% cell viability) was viewed as an acceptable level for the purposes of this study.

In D-283 cells, there was a moderate level of toxicity associated with the combination NPO6/TMZ treatment. There was minimal toxicity resulting from the NPO6 alone, and cell viability steadily declined as TMZ concentration increased. Viability did not drop below 20% for any concentration of TMZ.

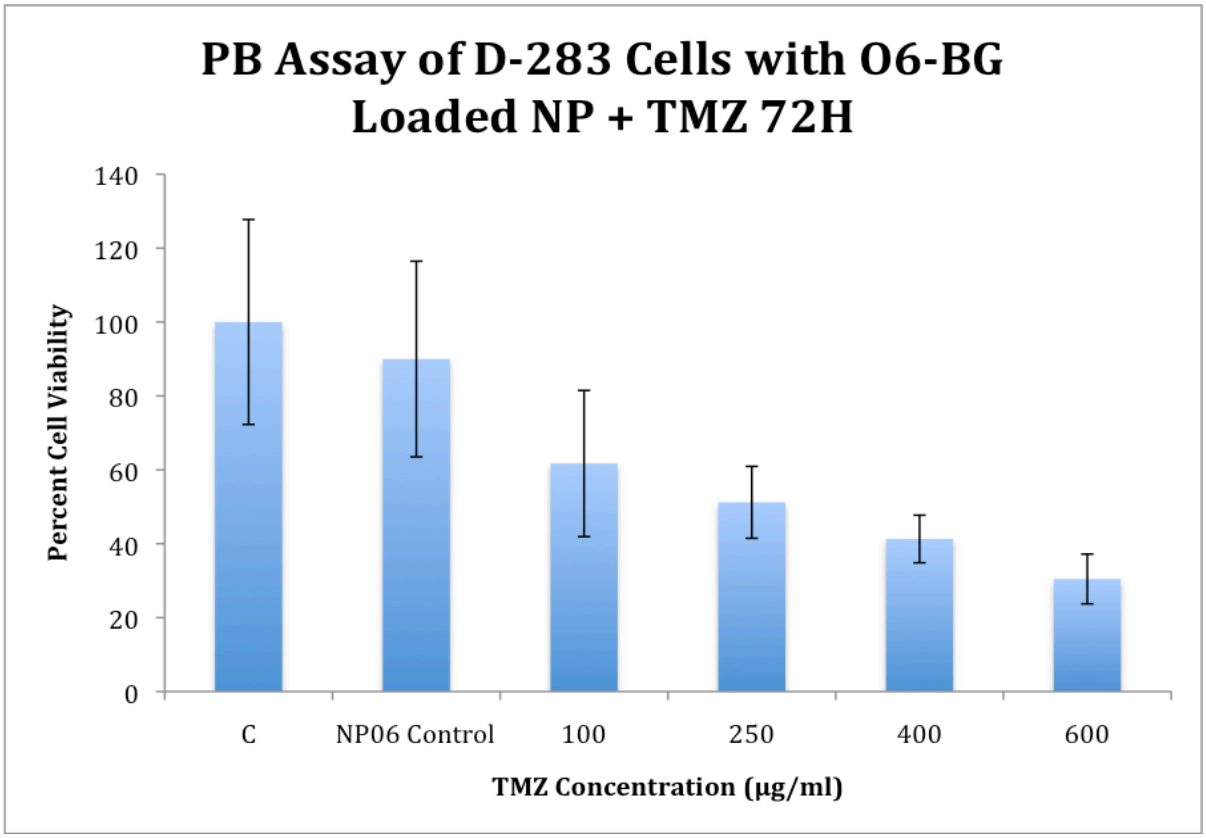

Figure 23 | Toxicity of O6-BG loaded nanoparticles & TMZ in D-283 cells. Cell viability below 60% indicates an acceptable toxicity level.

In Daoy cells, there was some toxicity observed. Viability remained around 60% for all concentrations of TMZ, while minimal toxicity was associated with only NPO6. At 100 µg/ml TMZ, there was also no toxicity observed, however, at 250 µg/ml, a steady decline in cell viability can be observed up to 600 µg/ml. Overall, the effect of this treatment on this cell line can be identified as 'moderate'.

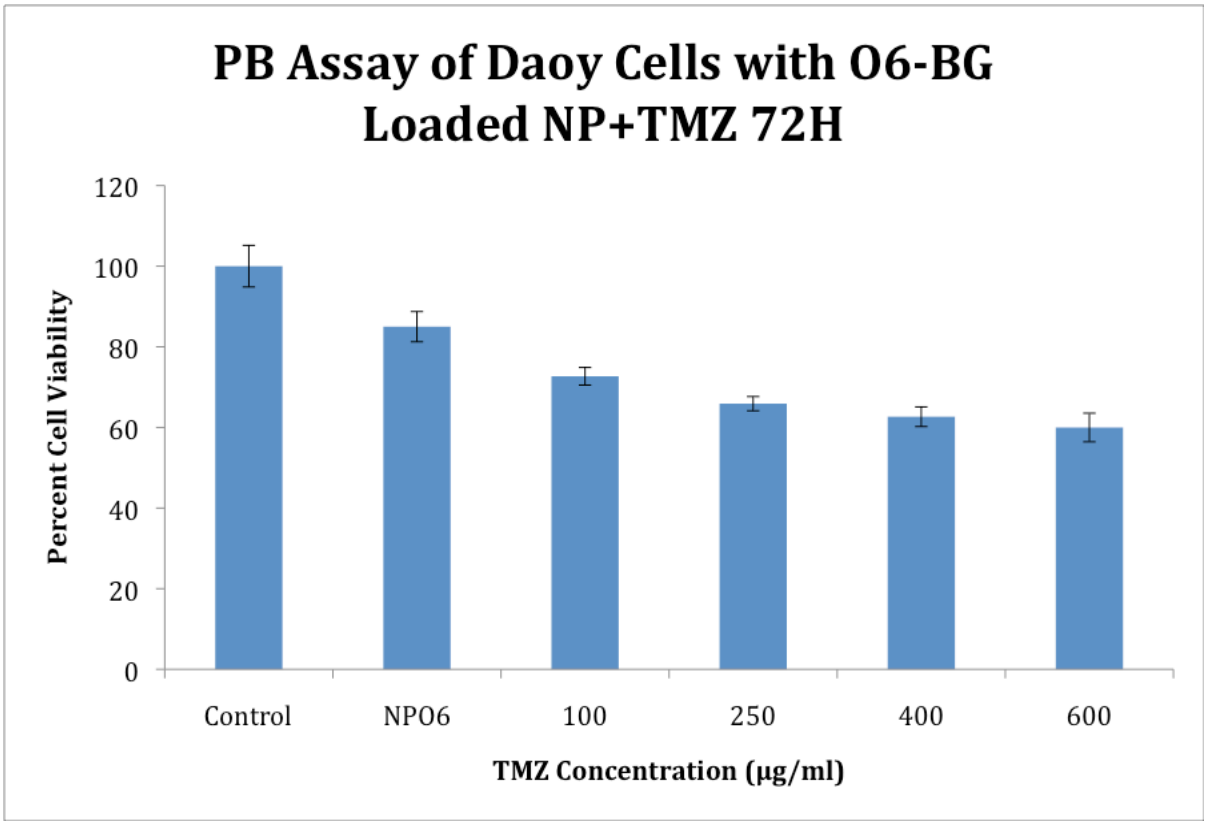

Figure 24 | Toxicity of O6-BG loaded nanoparticles & TMZ in Daoy cells. Cell viability below 60% indicates an acceptable toxicity level.

In SK-N-BE(2) cells, viability remained around 60% up to 250 µg/ml and dropped below 60% at 400 µg/ml, decreasing to around 40% at 600 µg/ml. There was also a slight toxic effect on the cells by the NPO6 alone.

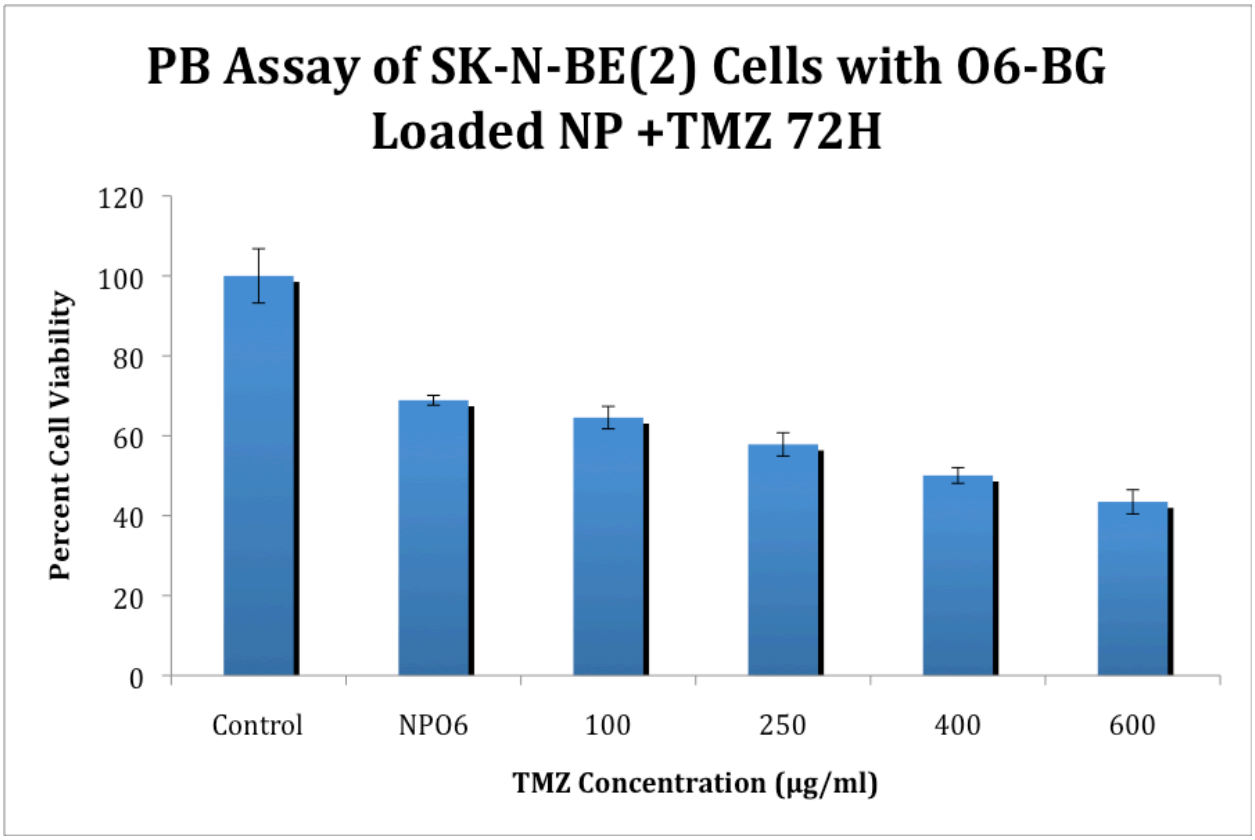

Figure 25 | Toxicity of O6-BG loaded nanoparticles & TMZ in SK-N-BE(2) cells. Cell viability below 60% indicates an acceptable toxicity level.

In SMS-KCNR cells, there was a significant level of toxicity associated with the combination NPO6+TMZ treatment. Cell viability remained around 60% from 100 to 250 µg/ml, and dropped below 60% at 400 µg/ml. Viability decreased dramatically to about 25% at 600 µg/mL TMZ concentration.

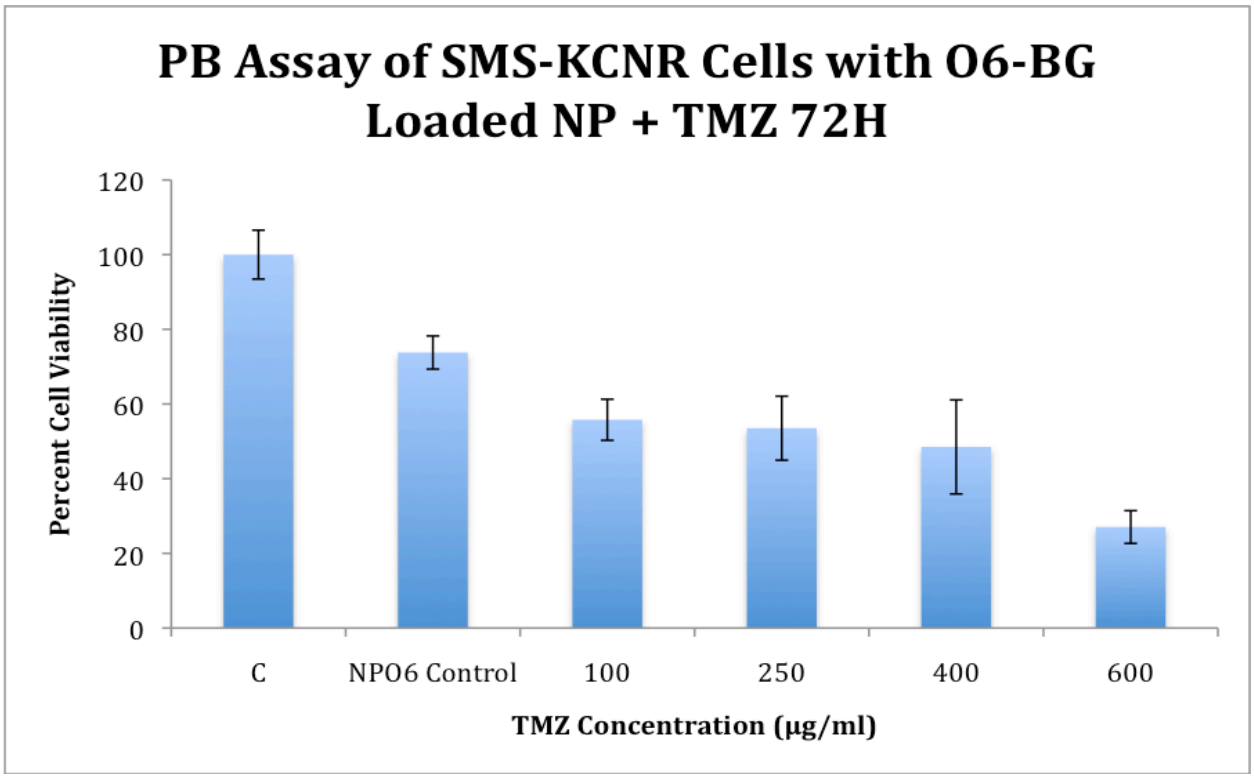

Figure 26 | Toxicity of O6-BG loaded nanoparticles & TMZ in SMS-KCNR cells. Cell viability below 60% indicates an acceptable toxicity level.

4.5.8. Combined Toxicity Data

The figures below show combined results of toxicity for each cell line. The graphs display cell viability at incubation periods varied from 24 to 72 hours from a series of free drug experiments as well as combination drug studies with free drug and nanoparticles loaded with O6-BG. The figures display the results of the following treatments: 128 µM TMZ, 256 µM TMZ, 64/128 µM O6-BG, 128 µM TMZ + 64/128 µM O6-BG, and 256 µM TMZ+64/128 µM O6-BG. Then, 600 µg/ml TMZ, 600 µg/ml TMZ+ 64/128 µM O6-BG, and 600 µM TMZ+ NPO6, with O6-BG loading at 2 mg/ml in the nanoparticles. The figures give a comprehensive view of the overall effect of each treatment on cell viability, and allow for analysis to determine whether the combination NPO6+TMZ treatment is indeed an effective method of treating neuroblastomas.

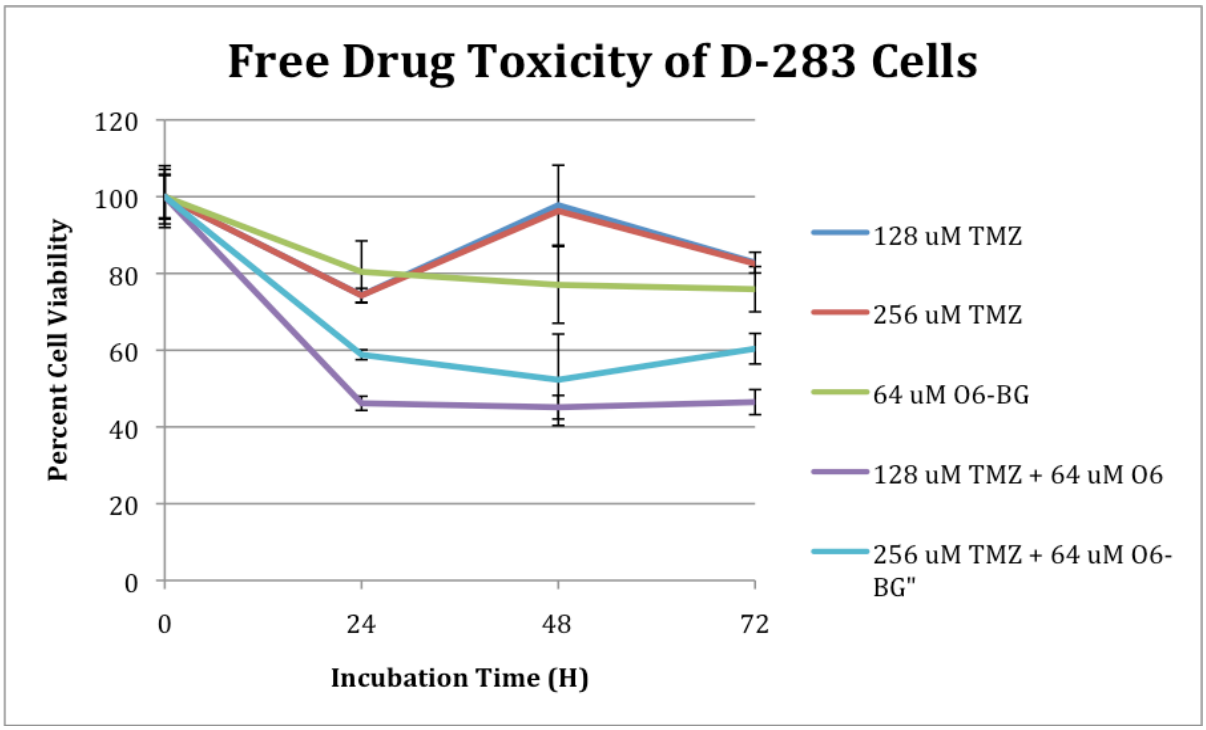

Figure 27 | Cell viability of 5 free drug toxicity tests on D-283 cells.

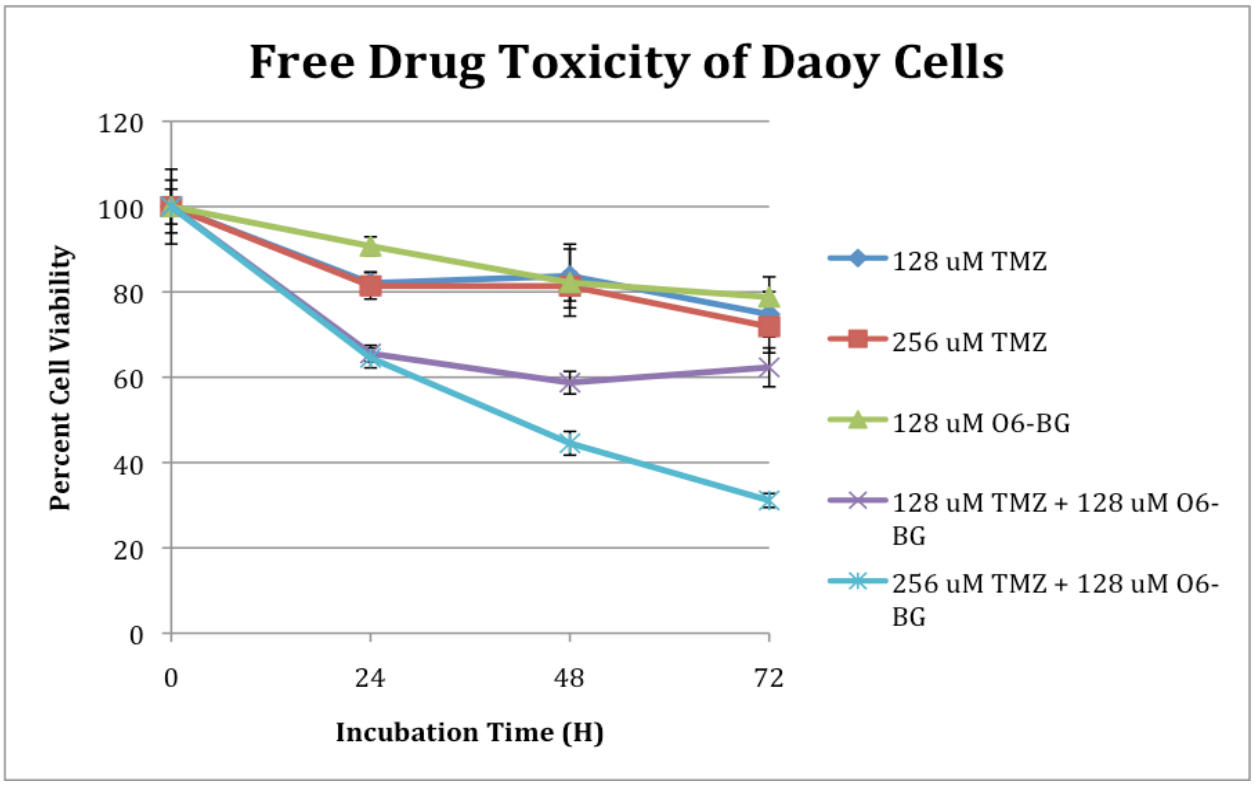

Figure 28 | Cell viability of 5 free drug toxicity tests on Daoy cells.

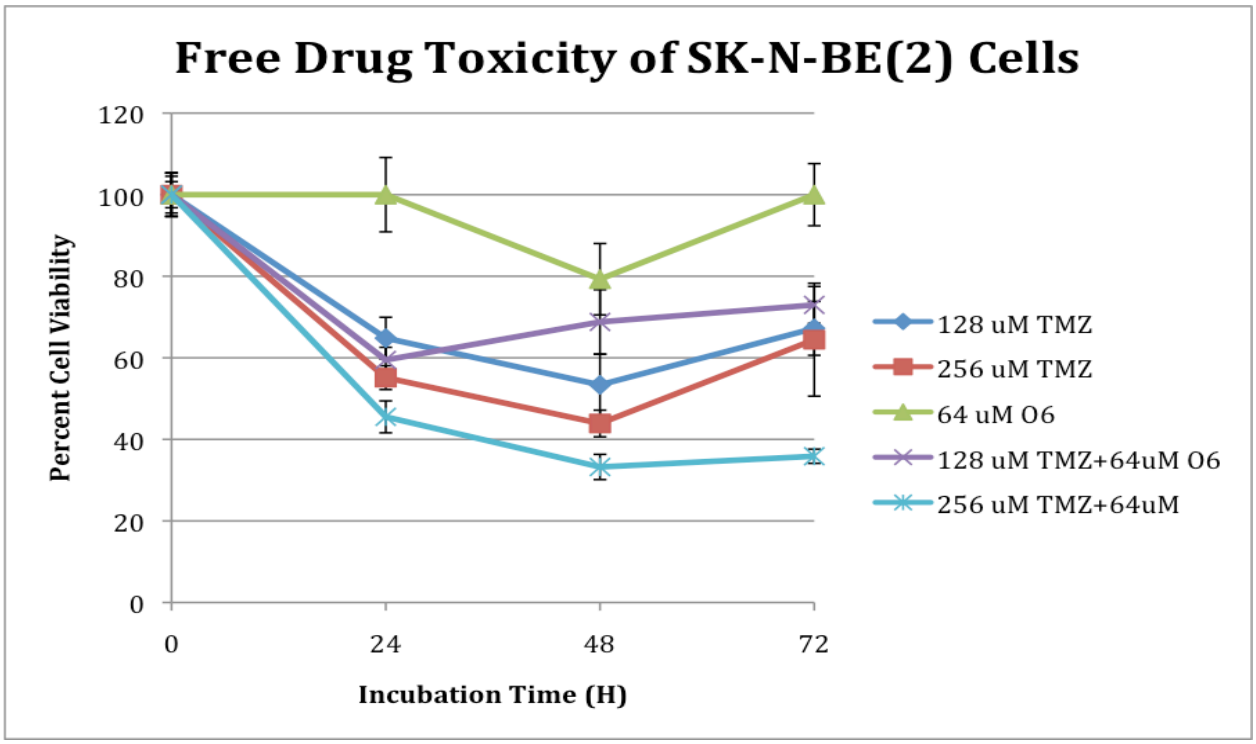

Figure 29 | Cell viability of 5 free drug toxicity tests on SK-N-BE(2) cells.

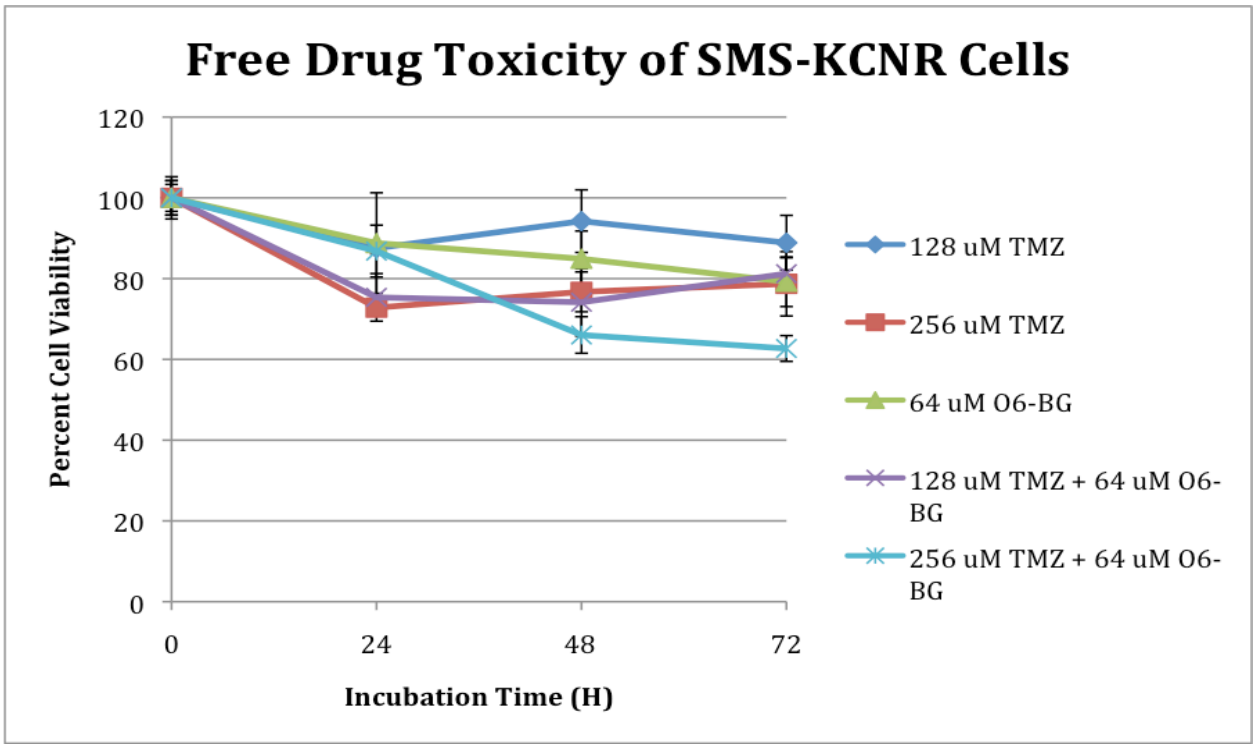

Figure 30 | Cell viability of 5 free drug toxicity tests on SMS-KCNR cells.

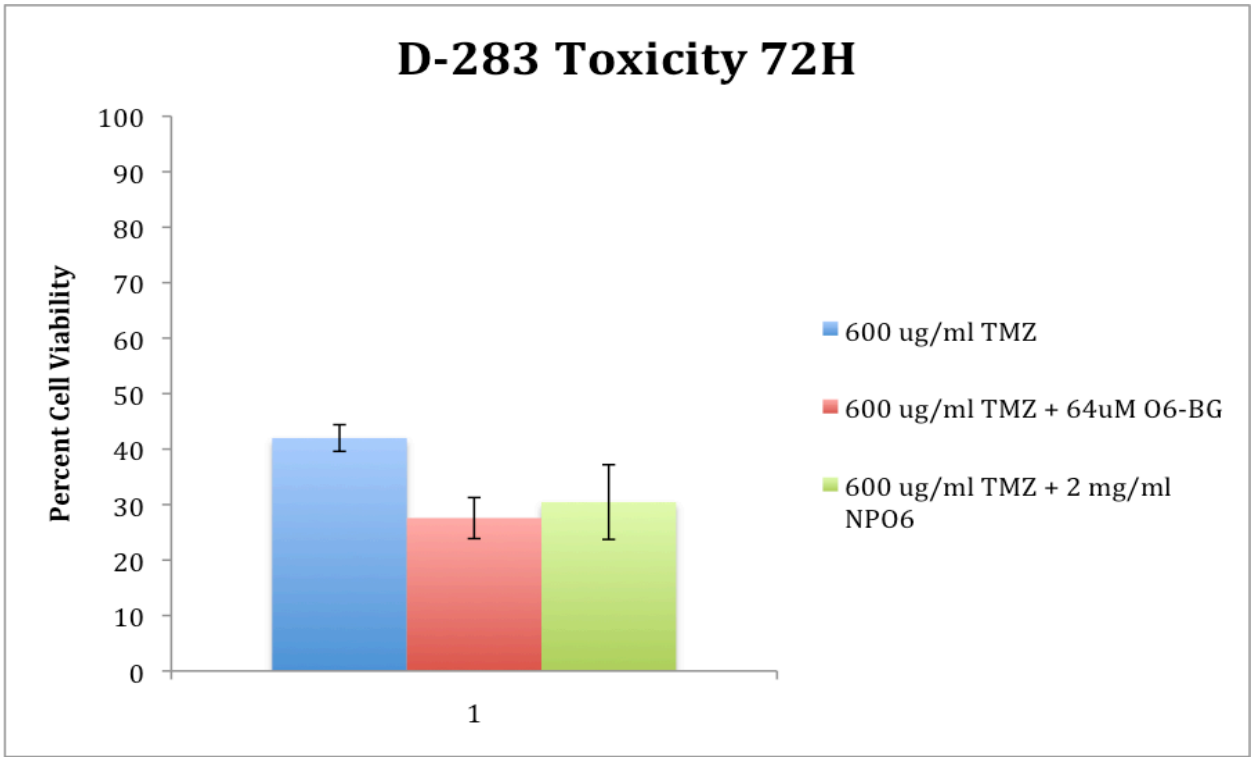

Figure 31 | Cell viability of 3 drug combination toxicity tests on D-283 cells.

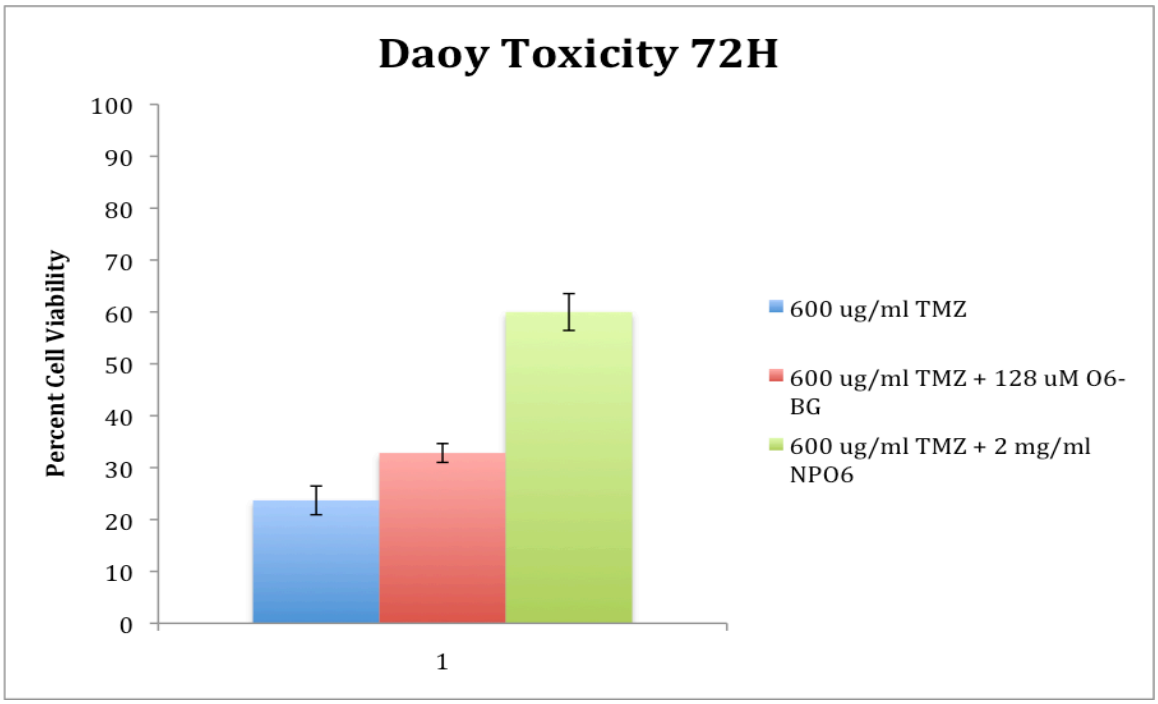

Figure 32 | Cell viability of 3 drug combination toxicity tests on Daoy cells.

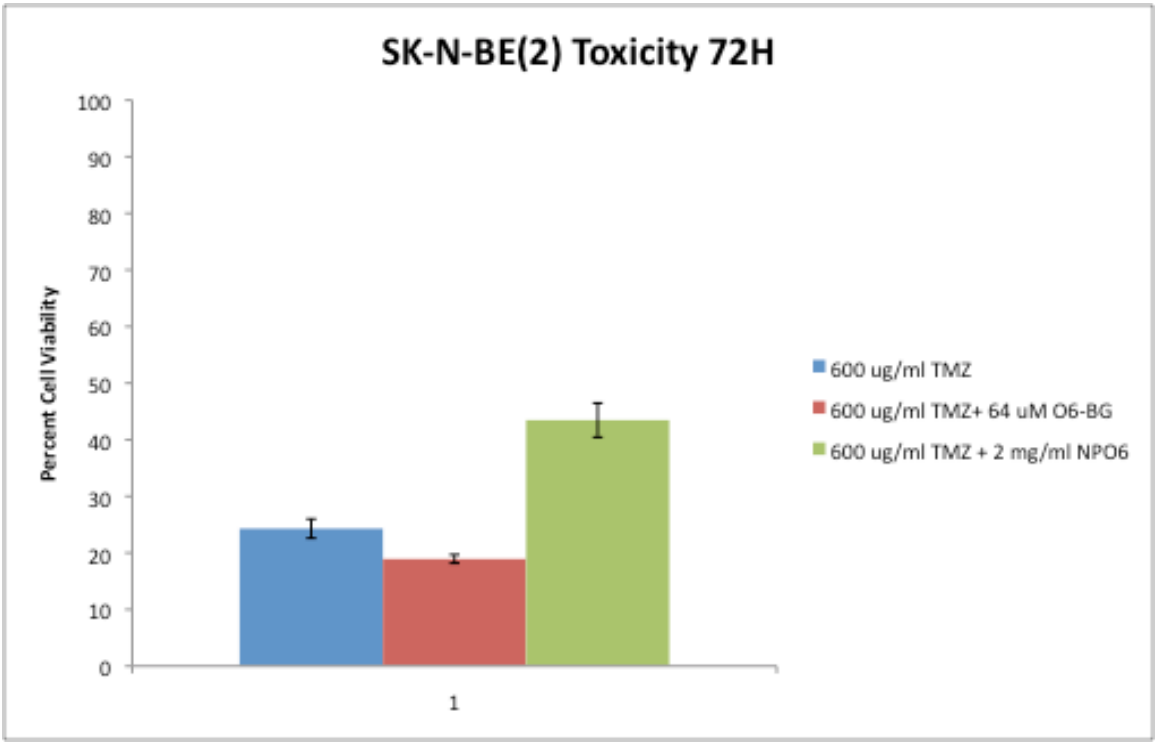

Figure 33 | Cell viability of 3 drug combination toxicity tests on SK-N-BE(2) cells.

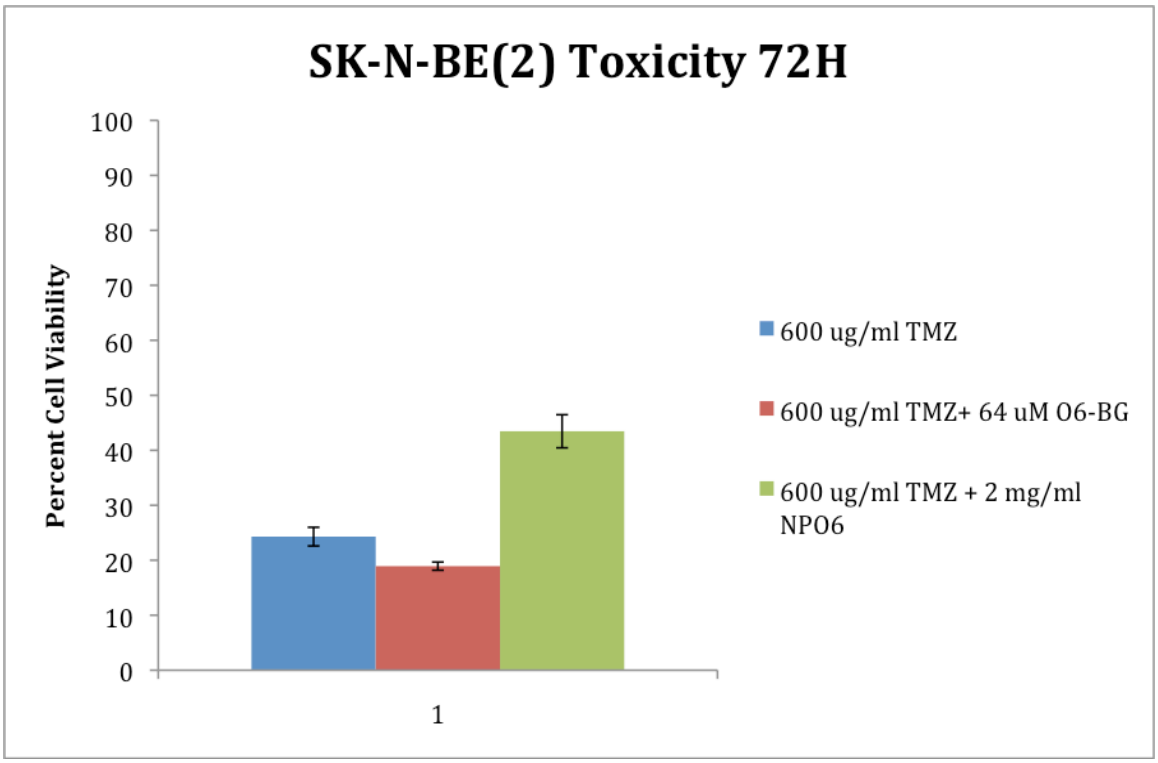

Figure 34 | Cell viability of 3 drug combination toxicity tests on SMS-KCNR cells.

4.5.8 Nanoparticle Uptake

Fluorescent nanoparticles were formulated to confirm that the nanoparticles were indeed uptaken into the cells. This study was carried out for 72 hours, with individual time points taken at 1 hour, 24 hours, 48 hours, and 72 hours. NP uptake into cells varied between cell lines, although all showed significant uptake after 24 hours. D-283 cells showed significant level of uptake after 24 hours, about 8-fold increase from 1 hour incubation.

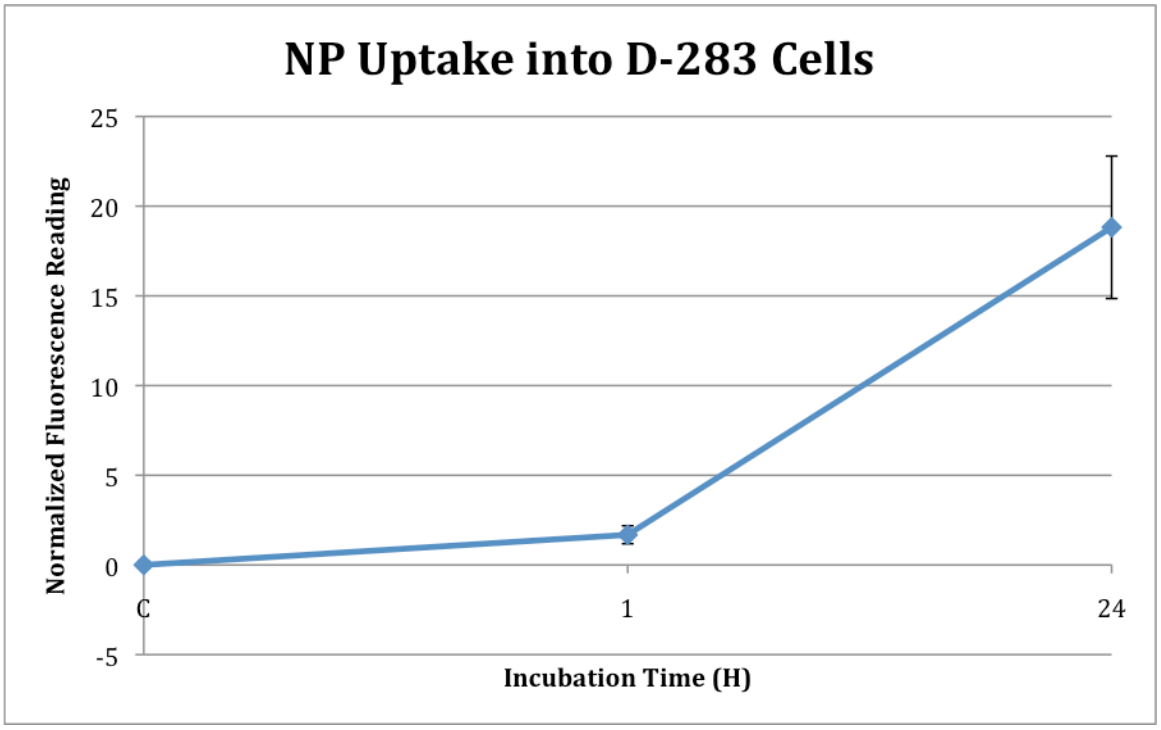

Figure 35 | NP Uptake into D-283 cells.

Daoy cells also successfully demonstrated cellular uptake up to 24 hours. There was about a 2.6 fold increase from 1 hour to 24 hours.

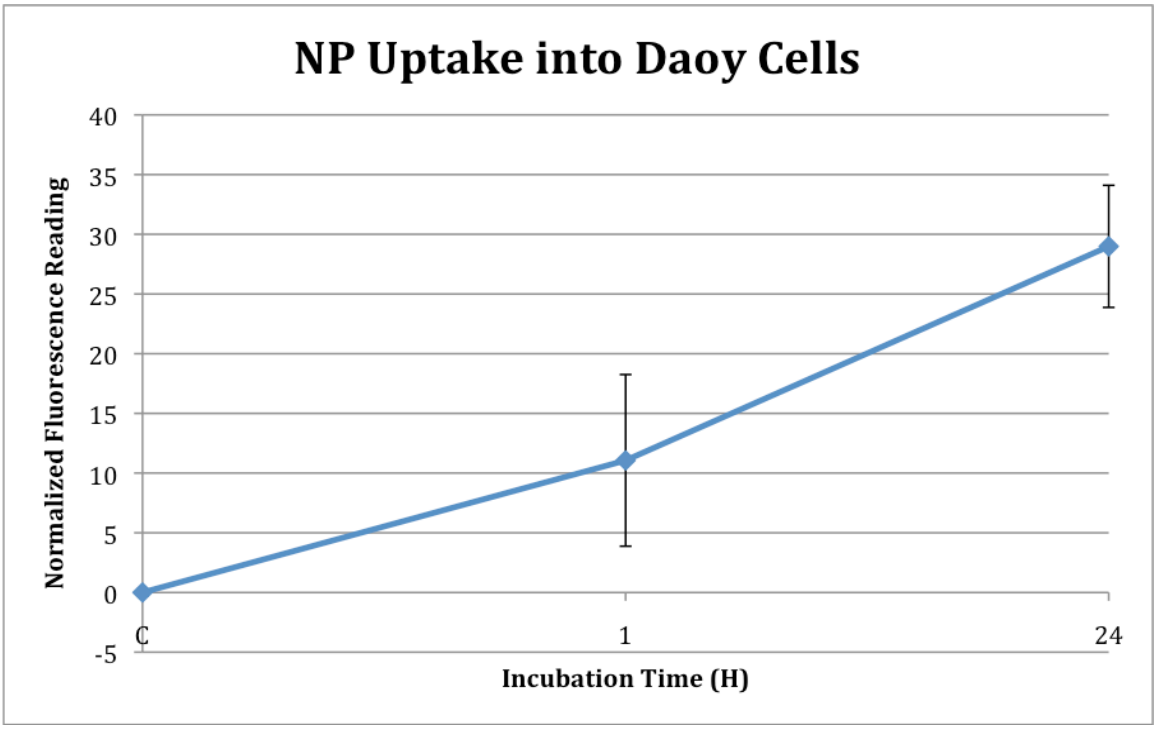

Figure 36 | NP Uptake into Daoy Cells.

SK-N-BE(2) cells showed an improved uptake level compared to D-283 and Daoy cells. There was a significant level of uptake up to 48 hours of incubation. Uptake levels increased 3.4 fold from 1 hour to 24 hours, and almost 4 fold from 24 hours to 48 hours, totaling more than 12 fold increase in uptake from 1 hour to 48 hours of incubation.

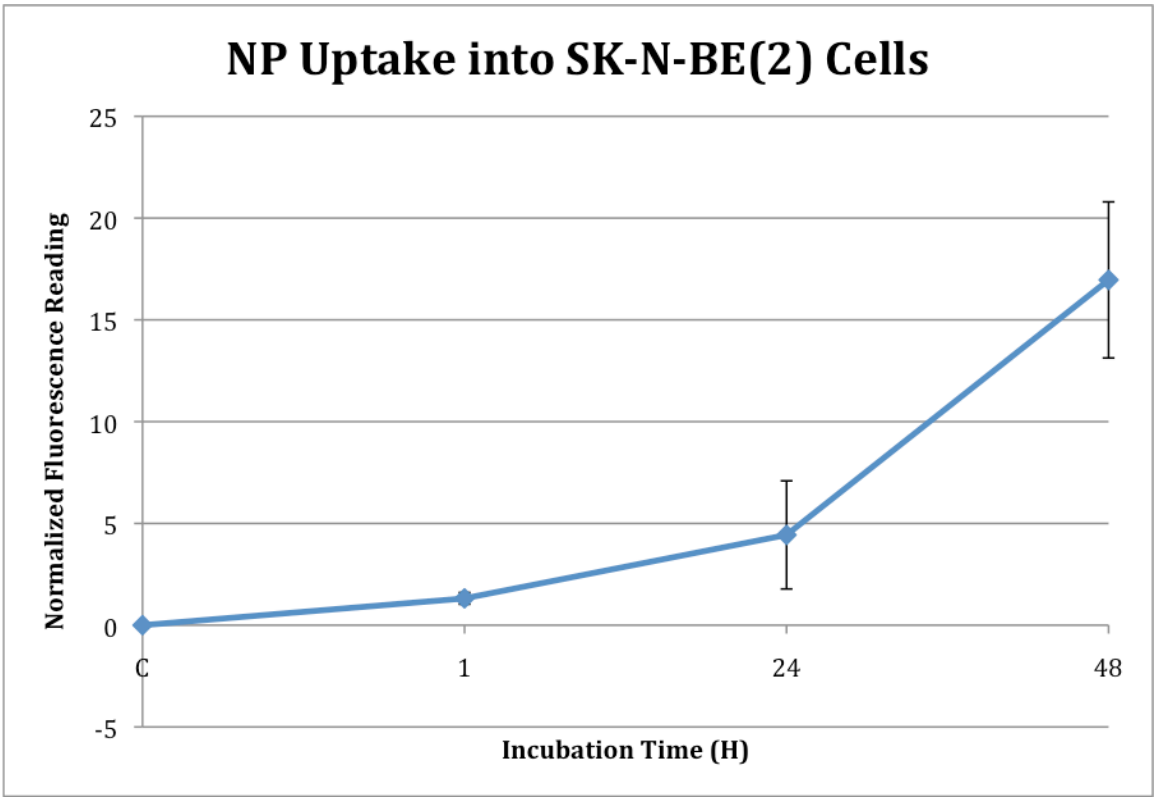

Figure 37 | NP Uptake into SK-N-BE(2) Cells.

SMS-KCNR cells showed increasing levels of uptake up to 72 hours, and it was the only cell line to do so. There was approximately 2.6 fold increase in uptake from 1 hour to 72 hours.

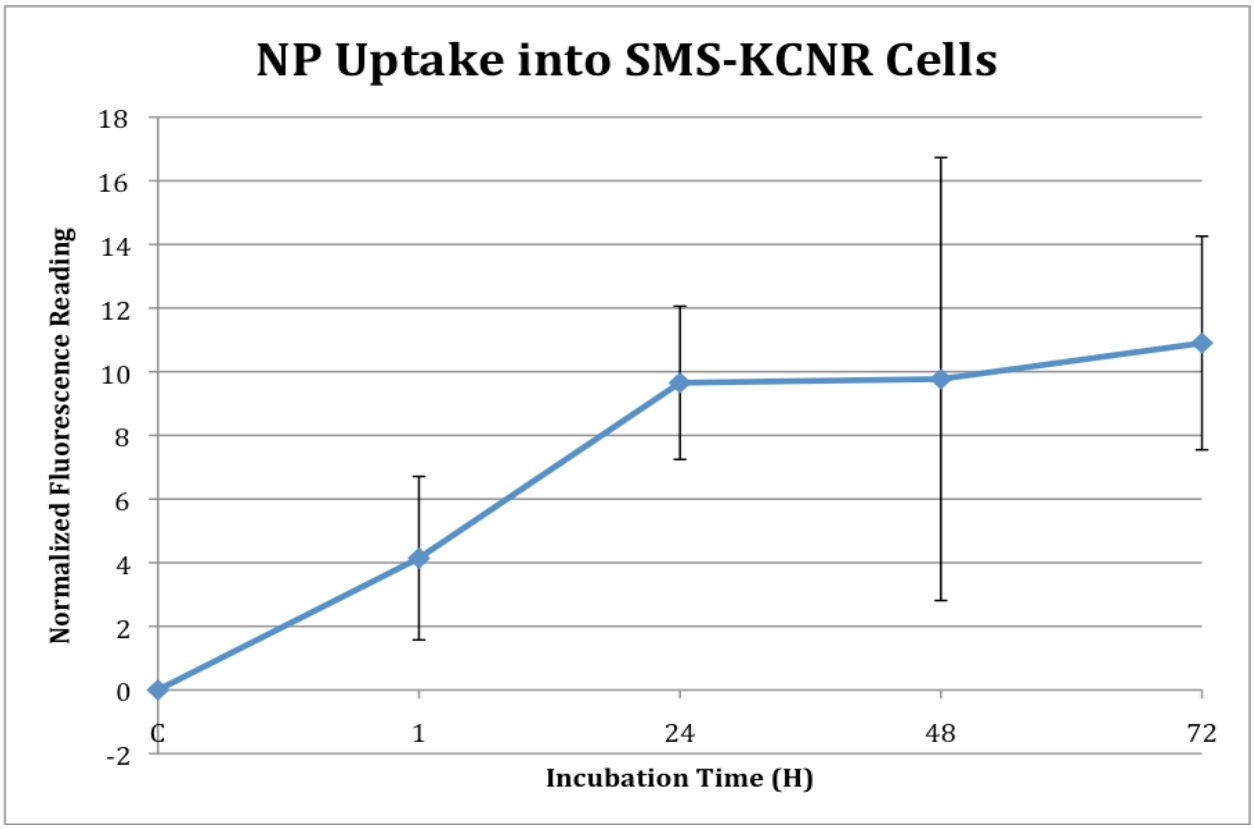

Figure 38 | NP uptake into SMS-KCNR Cells.

4.6. Conclusion of Results

The synthesis of PLA-PEG-(OCH_3) nanoparticles for the purpose of encapsulating and delivering drugs with controlled pharmacokinetics was achieved. Not only was the biocompatibility and non-toxicity of the nanoparticles demonstrated, but also the uptake of the nanoparticles into cells observed. This, along with the confirmed non-toxic properties of the MGMT-inhibitor O^6-BG, allows for an effective combination treatment with TMZ to enhance the toxicity and effectiveness of the drug in eliminating neuroblastoma cells. The results of the free TMZ studies showed that the drug is toxic to the cells, however, the effect of the drug resulted in very high toxicity levels indicating that the elevated concentrations administered are likely to be toxic to normal cells and tissues. The results of the free drug combination delivery of O^6-BG + TMZ also showed high toxicity levels, more enhanced in the cases of D-283, SK-N-BE(2), and SMS-KCNR cells than the free TMZ studies. However, once again the toxicity levels appeared extremely high which indicates that this treatment may be toxic to normal cells and tissues. The combination drug delivery of O^6-BG loaded nanoparticles (NPO6) with TMZ showed improved toxicity, however was lower compared to the free drug treatments. This can be explained by the fact that the drug loading in the NPO6+TMZ experiments was much lower than the free drug studies. The results show promise for a potential therapeutic system for the combination drug delivery using these nanoparticles.

CHAPTER 5

CONCLUSIONS

The 5-year survival rate for high-risk neuroblastoma is only 15%, which is evidence enough that the development of an effective treatment is extremely important. Presently, there are many treatment options that can treat the cancer, but not without side effects and the most challenging problem of drug resistance. Therefore, more focus must be placed on finding treatments that are more direct and target the tumor itself while avoiding normal cells. Nanoparticles are promising tools for delivering drugs due to their biocompatibility, ability to passively or directly target tumors, and controlled release of drugs to allow for lower dosage. These properties can effectively reduce side effects and systemic toxicity. Temozolomide is a commonly used therapeutic to treat neuroblastoma, but is inhibited from carrying out it's full function due to drug resistance induced by MGMT present in the cells. The co-administration of O^6-Benzylguanine with TMZ has the potential to be an effective method due to its ability to inhibit MGMT activity thereby allowing TMZ to fulfill its role in reducing the neuroblastoma cell viability. The results show that the encapsulation of O^6-BG into the PLA-PEG(OCH_3) nanoparticles was successful and co-administration with TMZ demonstrated a significant decrease in neuroblastoma cell viability without causing extreme levels of toxicity which could affect normal cells..

Overall, this combination drug nanoparticle delivery system shows strong potential for further development as a mechanism for the effective treatment of high-risk neuroblastoma.

CHAPTER 6

RECOMMENDATIONS FOR FUTURE RESEARCH

1. Attachment of targeting ligands such as peptides to the nanoparticles to target EGFR.

2. Analysis of drug loaded and unloaded nanoparticle uptake into 3D spheroid models, as well as toxicity studies in cell spheroids.

3. *In vivo* animal studies of drug loaded nanoparticles to examine uptake, drug release and biocompatibility.

REFERENCES

1. Neuroblastoma. *Natl Libr Med*. 2013. Available at: http://www.ncbi.nlm.nih.gov/pubmedhealth/PMH0002381/. Accessed May 18, 2014.

2. Cheung Nai-Kong V., and Michael A. Dyer. "Neuroblastoma: Developmental Biology, Cancer Genomics and Immunotherapy. *Nat Rev Cancer* 13 (2013): 397-411. Web. 22 June 2013.

3. "Neuroblastoma." *American Cancer Society*. American Cancer Society, 2012. Web. <http://www.cancer.org/cancer/neuroblastoma/detailedguide/index>.

4. Matthay, Katherin K., M.D, Judith G. Villablanca, M.D, Robert C. Seeger, M.D, Daniel O. Stram, Ph.D, Richard E. Harris, M.D, Norma K. Ramsay, M.D, Patrick Swift, M.D, Hiroyuki Shimada, M.D, Thomas C. Black, M.D, Garrett M. Brodeur, M.D, Robert B. Gerbing, M.A, and Patrick C. Reynolds, M.D., Ph.D. "Treatment of High-Risk Neuroblastoma with Intensive Chemotherapy, Radiotherapy, Autologous Bone Marrow Transplantation, and 13-Cis-Retinoic Acid." 341.16 (1999): 1165-172. Web. 9 Jan. 2014.

5. Neuroblastoma | Seattle Children's Hospital. Available at: http://www.seattlechildrens.org/medical-conditions/cancer-tumors/neuroblastoma/. Accessed May 15, 2014.

6. Wagner, Lars M., Roger E. McLendon, K. Jin Yoon, Brian D. Weiss, and Catherine A. Billups. "Targeting Methylguanine-DNA Methyltransferases in the Treatment of Neuroblastoma." *Clin Cancer Res* 13.18 (2007): 5418-424. Web.

7. Hans, M. L., and A. M. Lowman. "Biodegradable Nanoparticles for Drug Delivery and Targeting." *Current Opinion in Solid State and Materials Science* 6 (2002): 319-27. *Elsevier*. Web.

8. Magee, Jeffrey A., Elena Piskounova, and Sean J. Morrison. "Cancer Stem Cells: Impact, Heterogeneity, and Uncertainty." *Cancer Cell* 21 (2012): 283-92. Web. 24 June 2013.

9. Vlerken, Lilian E., and Mansoor M. Amiji. "Multi-functional Polymeric Nanoparticles for Tumour-Targeted Drug Delivery." *Expert Opinion* 3.2 (2006): 205-16. Web.

10. Peer, Dan, Jeffrey M. Karp, Seungpyo Hong, Omid C. Farokhzad, Rimona Margalit, and Robert Langer. "Nanocarriers as an Emerging Platform for Cancer Therapy." *Nature* 2 (2007): 751-60. Web.

11. Hu, Che-Ming J., Santosh Aryal, and Liangfang Zhang. "Nanoparticle-assisted Combination Therapies for Effective Cancer Treatment." *Therapeutic Delivery*1.2 (2010): 323-34. Web.

12. Esteller, Manel, Jesus Garcia-Foncillas, Esther Andion, Steven N. Goodman, Oscar F. Hidalgo, Vicente Vanaclocha, Stephen B. Baylin, and James G. Herman. "Inactivation of the DNA-Repair Gene MGMT and the Clinical Response of Gliomas to Alkylating Agents." *The New England Journal of Medicine* 343.19 (2000): 1350-354. Web.

13. Goldstein M, Roos WP, Kaina B. Apoptotic death induced by the cyclophosphamide analogue mafosfamide in human lymphoblastoid cells: contribution of DNA replication, transcription inhibition and Chk/p53 signaling. *Toxicol Appl Pharmacol.* 233(2008): 20-32.

14. Ludlum DB. "DNA alkylation by the haloethylnitrosoureas: Nature of Modifications Produced and their Enzymatic Repair or Removal. *Mutat Res* 233(1990): 117-126.

15. Fritz G, Tano K, Mitra S, Kaina B. "Inducibility of the DNA repair gene encoding O6-methylguanine-DNA methyltransferase in mammalian cells by DNA-damaging treatments." *Mol Cell Biol*. 11(1991): 4660-4668.

16. Kaina, Bernd, Geoffrey P. Margison, and Markus Christmann. "Targeting O6-methylguanine-DNA Methyltransferase with Specific Inhibitors as a Strategy in Cancer Therapy." *Cellular and Molecular Life Sciences* 67 (2010): 3663-681. Web.

17. Hazra TK, Roy R, Biswas T, Grabowski DT, Pegg AE, Mitra S. "Specific recognition of O6-methylguanine in DNA by active site mutants of human O6-methylguanine-DNA methyl- transferase." *Biochemistry* 36(1997):5769–5776.

18. Pegg AE, Dolan ME, Moschel RC. Structure, function, and inhibition of O6-alkylguanine-DNA alkyltransferase." *Prog Nucleic Acid Res Mol Biol* 51(1995):167–223.

19. Dolan ME, Mitchell RB, Mummert C, Moschel RC, Pegg AE. "Effect of O6-benzylguanine analogues on sensitivity of human tumor cells to the cytotoxic effects of alkylating agents." *Cancer Res.* 51(1991): 3367-3372.

20. Schold SC Jr, Kokkinakis DM, Chang SM, Berger MS, Hess KR, Schiff D, Robins HI, Mehta MP, Fink KL, Davis RL, Prados MD. “O6-benzylguanine suppression of O6-alkyl- guanine-DNA alkyltransferase in anaplastic gliomas.” *Neuro Oncol* 6(2004):28–32.

21. Spiro TP, Gerson SL, Liu L, Majka S, Haaga J, Hoppel CL, Ingalls ST, Pluda JM, Willson JK. “O6-benzylguanine: a clinical trial establishing the biochemical modulatory dose in tumor tissue for alkyltransferase-directed DNA repair.” *Cancer Res* 59 (1999):2402–2410.

22. Warren KE, Aikin AA, Libucha M, Widemann BC, Fox E, Packer RJ, Balis FM. “Phase I study of O6-benzylguanine and temozolomide administered daily for 5 days to pediatric patients with solid tumors.” *J Clin Oncol* 23(2005):7646–7653.

23. Dolan, M. E., and Anthony E. Pegg. "O6-Benzylguanine and Its Role in Chemotherapy." *Clinical Cancer Research* 3 (1997): 837-47. Print.

24. Herve, Rubie, Julia Chisholm, Anne S. Defachelles, Bruce Morland, and Caroline Munzer. "Phase II Study of Temozolomide in Relapsed or Refractory High-Risk Neuroblastoma." *Journal of Clinical Oncology* 24.33 (2006): 5259-264. Web.

25. Cai, W., N. V. Maldonado, W. Cui, N. Harutyunyan, L. Ji, R. Sposto, C. P. Reynolds, and N. Keshelava. "Activity of Irinotecan and Temozolomide in the Presence of O6-methylguanine-DNA Methyltransferase Inhibition in Neuroblastoma Pre-Clinical Models." *British Journal of Cancer* 103 (2010): 1369-379. Web.

26. Zhang, L., F. X. Gu, J. M. Chan, A. Z. Wang, R. S. Langer, and O. C. Farokhzad. "Nanoparticles in Medicine: Therapeutic Applications and Developments." *Clinical Pharmacology & Therapeutics*83.5 (2008): 761-67. Web.

27. Jain, Rakesh K., and Triantafyllos Stylianopoulos. "Delivering Nanomedicine to Solid Tumors." *Nat Rev Clin Oncol* 7.11 (2010): 653-64. Web.

28. Wang, Andrew Z., Robert Langer, and Omid C. Farokhzad. "Nanoparticle Delivery of Cancer Drugs." *Annual Review of Medicin* 63 (2012): 185-98. Web.

29. Wilczewska, Agnieszka Z., Katarzyna Niemirowicz, Karolina H. Markiewicz, and Halina Car. "Nanoparticles as Drug Delivery Systems. "*Pharmacological Reports* 64 (2012): 1020-037. Web.

30. Mattix, Brandon, Thomas Moore, Olga Uvarov, Samuel Pollard, Lauren O'Donnell, Katelyn Park, Devante Horne, Jhilmil Dhulekar, Laura Reese, Duong Nguyen, Jacqueline Kraveka, Karen Burg, Frank Alexis. "Effects of Polymeric Nanoparticle Surface Properties on Interaction with Brain Tumor Environment." *Nano LIFE.* 2010:1(1).

31. Wang B, Jiang W, Yan H, et al. "Novel PEG-graft-PLA nanoparticles with the potential for encapsulation and controlled release of hydrophobic and hydrophilic medications in aqueous medium." *Int J Nanomedicine*. (6)2011:1443-1451.Web.

32. Kamaly, Nazila, Pedro M. Valencia, Aleksandar F. Radovic-Moreno, and Omid C. Farokhzad. "Targeted Polymeric Therapeutic Nanoparticles: Design, Development and Clinical Translation."*Chem.Soc.Rev* 41 (2012): 2971-3010. Print.

33. Silber, John R., A. Blank, and Michael S. Bobola. "O6-Methylguanine-DNA Methyltransferase-deficient Phenotype in Human Gliomas: Frequency and Time to Tumor Progression after Alkylating Agent-based Chemotherapy." *Clinical Cancer Research* 5 (1999): 807-14. *American Association for Cancer Research.* Web. 30 May 2014.

34. Liu, Lili, and Stanton L. Gerson. "Targeted Modulation of MGMT: Clinical Implications." *Clinical Cancer Research* 12.2 (2006): 328-31. *American Association for Cancer Research*. Web. 27 May 2014.

35. Alexis, Frank. "Factors Affecting the Degradation and Drug-release Mechanism of Poly(lactic Acid) and Poly[(lactic Acid)-co-(glycolic Acid)]." *Polymer International* 54.1 (2004): 36-46. Web.

36. Alexis, Frank, Eric Pridgen, Linda K. Molnar, and Omid C. Farokhzad. "Factors Affecting the Clearance and Biodistribution of Polymeric Nanoparticles." *Molecular Pharmaceutics* 5.4 (2008): 505-15. Web.

37. Christmann, Markus, Barbara Verbeek, Wynand P. Roos, and Bernd Kaina. "O(6)-Methylguanine-DNA Methyltransferase (MGMT) in Normal Tissues and Tumors: Enzyme Activity, Promoter Methylation and Immunohistochemistry." *Biochimica et Biophysica Acta* 1816.2 (2011): 179-90. *Elsevier*. Web.

38. Herfarth, K. K., T. P. Brent, R. P. Danam, J. S. Remack, I. J. Kodner, S. A. Wells, Jr., and P. J. Goodfellow. "A Specific CpG Methylation Pattern of the MGMT Promoter Region Associated with Reduced MGMT Expression in Primary Colorectal Cancers." *Molecular Carcinogenesis*24.2 (1999): 90-98. *PubMed*. Web.

39. Bobola, Michael S., A. Blank, Mitchel S. Berger, and John R. Silber. "O6-Methylguanine-DNA Methyltransferase Deficiency in Developing Brain: Implications for Brain Tumorigenesis." *DNA Repair (Amst)* 6.8 (2007): 1127-133. *NIH-PA*. Web.

40. Houghton, P., C. Stewart, and P. Cheshire et al. "Antitumor Activity of Temozolomide Combined with Irinotecan Is Partly Independent of O6-Methylguanine-DNA Methyltransferase and Mismatch Repair Phenotypes in Xenograft Models." *Clinical Cancer Research* 6 (2000): 4110-118. Web.